MOX–Report No. 7/2009

An efficient generalization of the Rust-Larsen method for solving electro-physiology membrane equations

Mauro Perego, Alessandro Veneziani

MOX, Dipartimento di Matematica "F. Brioschi"
Politecnico di Milano, Via Bonardi 9 - 20133 Milano (Italy)

mox@mate.polimi.it http://mox.polimi.it

An efficient generalization of the Rush-Larsen method for solving electro-physiology membrane equations

Mauro Perego[♯,*], Alessandro Veneziani[*]

January, 28, 2009

[♯] MOX– Modellistica e Calcolo Scientifico
Dipartimento di Matematica "F. Brioschi"
Politecnico di Milano
via Bonardi 9, 20133 Milano, Italy
mauro.perego@polimi.it
[*]Department of Mathematics and Computer Science
Emory University
400 Dowmann Drive, 30322 Atlanta (GA), USA

Keywords: electro-physiology, ionic models, Rush-Larsen scheme, time-adaptivity, Monodomain, Bidomain.

AMS Subject Classification: 65M12, 65L05, 35K65

Abstract

In this paper we address a second-order class of methods for solving ordinary differential systems coming from some problems in electro-physiology. The set of methods generalizes to the second order a previous proposal by Rush and Larsen (1978). We prove that the methods are second-order convergent and are in general more stable than the corresponding multistep methods. Moreover, they feature better positivity properties. We present their time-adaptive formulation, which is well suited for our electrophysiology problems. In particular, numerical results are presented on the Monodomain model coupled to Luo-Rudy I ionic models for the propagation of the cardiac potential.

1 Introduction and motivations

In this paper we propose a numerical method designed to solve systems of Ordinary Differential Equations (ODEs) coming form cell-membrane models for ionic currents and voltages. Starting from the Hodgkin-Huxley model [9], developed in 1952 to describe the action potential in giant squid axons, several cell-membrane

models have been developed, in particular for cardiac cells. We mention, for instance, the Beeler-Reuter model [1], the Luo-Rudy phase I model [14] and the Winslow model [12] developed for the ventricular cells and the Courtemanche model [3] for the atrial cells. All these models can be written in terms of the transmembrane potential u, the vector of the gating variables $\mathbf{w}$ and the vector of the ionic concentrations $\mathbf{X}$, as described in the following system:

$$\begin{cases} \dfrac{\partial u}{\partial t} = I(t, u, \mathbf{X}, \mathbf{w}) \\ \dfrac{\partial w_i}{\partial t} = a_i(u) w_i + b_i(u) \quad i = 1, \ldots, m, \\ \dfrac{\partial \mathbf{X}}{\partial t} = \mathbf{g}(u, \mathbf{X}, \mathbf{w}) \end{cases} \tag{1}$$

for $t \in (0, T]$, with initial conditions $u(0) = u^0$, $\mathbf{w}(0) = \mathbf{w}^0$ and $\mathbf{X}(0) = \mathbf{X}^0$. $I(t, u, \mathbf{X}, \mathbf{w})$ is the source term defined as

$$I(t, u, \mathbf{X}, \mathbf{w}) = \frac{1}{C_m} \left(I_{app}(t) - I_{ion}(u, \mathbf{X}, \mathbf{w}) \right),$$

being C_m the membrane capacity, I_{app} an applied current stimulus and I_{ion} the ionic current. I_{ion}, $\mathbf{g}$, $\boldsymbol{a}$, $\boldsymbol{b}$, u_0, $\mathbf{w}_0$ and $\mathbf{X}_0$ depend on the specific ionic model (in the case of Luo-Rudy phase I model see Appendix for functions and parameters definitions and Figure 1 for the graphs of the variables). Parameters $\boldsymbol{a}$ and $\boldsymbol{b}$ and variable $\mathbf{w}$ fulfill the following inequalities: $a_i < 0$, and $\left(-\dfrac{b_i}{a_i} \right) \in [0, 1]$, and $\mathbf{w}_i^0 \in [0, 1]$ for $i = 1, \ldots, m$. This implies (see Sect. 3.4) that $w_i \in [0, 1]$. Typically, system (1) is stiff and the gating variables feature high gradients. The most popular method for solving this system is the simple first order scheme proposed by Rush and Larsen [18] which guarantees that the numerical solutions for gating variables are in the range [0, 1]. In the same paper Rush and Larsen proposed a very simple time adaptive algorithm, based only on the values of $\dfrac{\partial u}{\partial t}$. Another popular way to solve system (1) is to use the more complex Runge-Kutta (RK) schemes.In this paper we propose a second order extension of Rush-Larsen scheme and a time adaptive strategy based on predictor-corrector error estimates.

In electro-cardiology, in order to simulate the action potential propagation in the myocardium, ionic models are coupled with the so called Monodomain or Bidomain systems of Partial Differential Equations (PDEs). For an introduction to Electrocardiology models see [16]. Monodomain and Bidomain systems are commonly discretized using an IMplicit-EXplicit (IMEX) approach for the PDEs and the Rush-Larsen scheme for the ionic model (see [5]). In [19] a second order method based on an operator-splitting technique was proposed for the time discretization of the PDEs, while a RK scheme was used for discretizing the ionic model. More complex time and space adaptive methods are presented in [4], [22]

and [2]. In this paper we introduce a simple second order IMEX scheme combined with our extension of Rush-Larsen scheme for the ionic model. Also, we extend the adaptive strategy presented for the ionic model to the electro-cardiology problem. One dimensional simulations, using Finite Element discretization, are reported for the solution of Monodomain system, illustrating the effectiveness of our method.

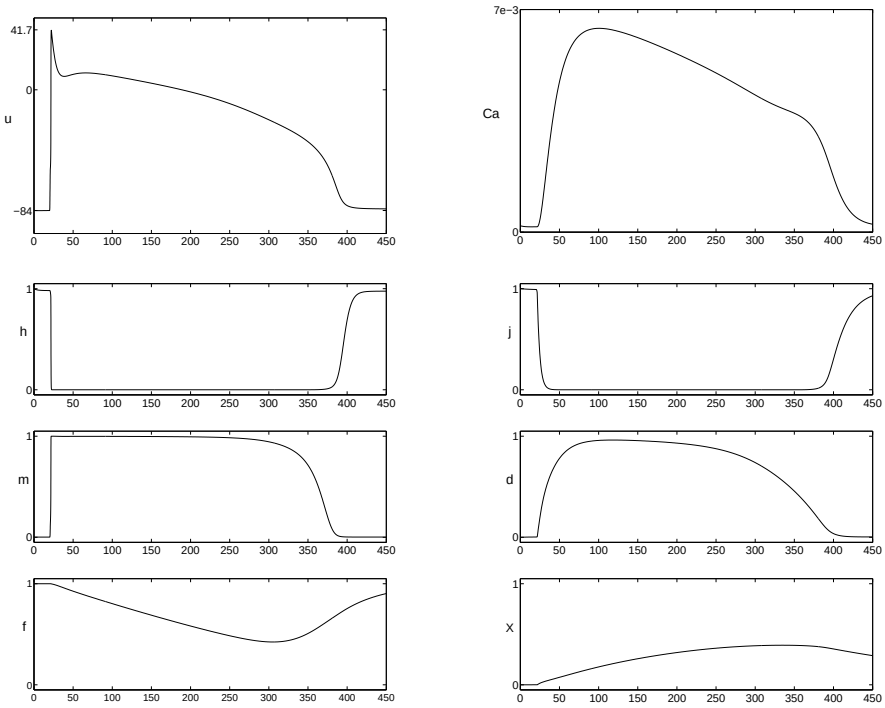

Figure 1: Variables of Luo-Rudy model as functions of time (in ms): transmembrane potential u (mV) and intracellular calcium Ca (M) in the first row, the gating variables h, j, m, d, f and x in the last three rows.

The outline of the paper is as follows. In Sect. 2 we recall the Rush-Larsen method and present our extension. Sect. 3 is devoted to the theoretical analysis of the new method; we derive convergence results, absolute stability regions and positivity properties. Our scheme can be addressed as a generalization of first and second order multistep methods. We prove that our generalization guarantees better properties of stability and positivity. Sect. 4 presents some practical details in using the new scheme for the electro-physiology equations. Sect. 5 presents the time-adaptive formulation of our method. Numerical results for the Monodomain problem in electro-cardiology.

Throughout the paper, bold characters will denote vectors.

2 The scheme

Let us start considering the following initial value problem:

$$\begin{cases} \dfrac{\partial y_i}{\partial t} = f(t,\mathbf{y}) = \mathtt{a}_i(t,\mathbf{y})\, y_i + \mathtt{b}_i(t,\mathbf{y}), \quad i = 1,\dots,m \quad t \in (0,T] \\ \mathbf{y}^0 = \mathbf{y}(0). \end{cases} \tag{2}$$

Given a generic non-linear ordinary differential system, there are clearly many different ways for recasting it in the form (2). In the applications, the identification of $\mathtt{a}$ and $\mathtt{b}$ is driven by the problem at hand (see (1)). In general, there is no trivial way for writing $\mathbf{f}$ in the form $f_i = \mathtt{a}_i y_i + \mathtt{b}_i$, so that it makes sense to distinguish the two vectors $\mathtt{a}$ and $\mathtt{b}$. A particular class of problems, for which a specific choice of the coefficients $\mathtt{a}$ and $\mathtt{b}$ leads to good positivity properties, is analyzed in Sect. 3.4.

Rush and Larsen [18] proposed the following numerical scheme for the solution of the previous system:

$$\begin{cases} y_i^{n+1} = e^{\mathtt{a}_i^n h}\left(y_i^n + \dfrac{\mathtt{b}_i^n}{\mathtt{a}_i^n}\right) - \dfrac{\mathtt{b}_i^n}{\mathtt{a}_i^n}, \quad n = 0,\dots,N, \quad i = 1,\dots,m \\ \mathbf{y}^0 = \mathbf{y}(0), \end{cases} \tag{3}$$

where $\mathbf{y}^n$ is the approximation of the solution $\mathbf{y}(t^n)$, being $t^n = n\,h$, $T = Nh$ and $h > 0$ the time step. Vectors with entries $\mathtt{a}_i$ and $\mathtt{b}_i$ are denoted by $\mathbf{a}$ and $\mathbf{b}$. More precisely, $\mathbf{a}^n$ and $\mathbf{b}^n$ are defined as $\mathbf{a}^n = \mathbf{a}(t^n, \mathbf{y}^n)$ and $\mathbf{b}^n = \mathbf{a}(t^n, \mathbf{y}^n)$ respectively. This method stems from considering functions $\mathbf{a}$ and $\mathbf{b}$ constant on the interval $(t^n,\, t^{n+1}]$ and equal to $\mathbf{a}^n$ and $\mathbf{b}^n$; $\mathbf{y}^{n+1}$ is the exact solution at time t^{n+1} of the linearized differential system

$$\begin{cases} \dfrac{\partial \tilde{y}_i}{\partial t} = \mathtt{a}_i^n \tilde{y}_i + \mathtt{b}_i^n, \quad t \in (t^n, t^{n+1}] \\ \tilde{\mathbf{y}}(t^n) = \mathbf{y}^n, \end{cases} \tag{4}$$

for $i = 1,\dots,m$ and $n = 0,\dots N$. This is an explicit scheme and however it allows us to take a time-step significantly greater than the one of the Forward Euler (FE) scheme in order to avoid numerical instability. For instance, when solving the Luo-Rudy model in the cases presented in Sect. 4, we found that FE is stable with time-steps $\leq 0.01\ ms$, while Rush-Larsen is stable for $h \leq 0.1\ ms$. Moreover the computed values of the gating variables belong to the range [0, 1] in the Rush-Larsen case, while do not in the FE case, for large values of h. We will give an explanation of these evidences in Sections 3.3 and 3.4. Unfortunately, the original Rush-Larsen scheme is only first order accurate. Our goal is to devise a second order extension to this scheme. We start rewriting scheme (3) in the following form,

$$\begin{cases} y_i^{n+1} = e^{\mathtt{a}_i^n h} y_i^n + h\Phi(\mathtt{a}_i^n h)\mathtt{b}_i^n = y_i^n + h\Phi(\mathtt{a}_i^n h)(\mathtt{a}_i^n y_i^n + \mathtt{b}_i^n), \\ \mathbf{y}^0 = \mathbf{y}(0); \end{cases} \tag{5}$$

for $i = 1, \dots, m$ and $n = 0, \dots N$, with

$$\Phi(x) = \begin{cases} \dfrac{e^x - 1}{x} & x \neq 0, \\ 1 & x = 0. \end{cases}$$

For $\mathbf{a} = 0$ the scheme reduces to the Forward Euler (FE) scheme.

In order to increase the accuracy of the Rush-Larsen scheme we evaluate the coefficients $\mathbf{a}$ and $\mathbf{b}$ at $t^{n+\frac{1}{2}}$, namely

$$\begin{cases} y_i^{n+1} = y_i^n + h\Phi(\mathtt{a}_i^{n+\frac{1}{2}}h)(\mathtt{a}_i^{n+\frac{1}{2}}\, y_i^n + \mathtt{b}_i^{n+\frac{1}{2}}), \quad n = 0, \dots, N, \quad i = 1, \dots, m \\ \mathbf{y}^0 = \mathbf{y}(0); \end{cases} \tag{6}$$

where $\mathbf{a}^{n+\frac{1}{2}}$ and $\mathbf{b}^{n+\frac{1}{2}}$ are approximations of $\mathbf{a}(t^{n+\frac{1}{2}})$ and $\mathbf{b}(t^{n+\frac{1}{2}})$. In particular, we select for $n = 1, \dots, N$,

$$\begin{array}{l} \mathbf{a}^{n+\frac{1}{2}} = c_{-1}\mathbf{a}^{n+1} + c_0\mathbf{a}^n + c_1\mathbf{a}^{n-1} \quad , \mathbf{b}^{n+\frac{1}{2}} = c_{-1}\mathbf{b}^{n+1} + c_0\mathbf{b}^n + c_1\mathbf{b}^{n-1}, \\ \mathbf{a}^{\frac{1}{2}} = c_{-1}\mathbf{a}^1 + (c_0 + c_1)\mathbf{a}^0 \quad , \mathbf{b}^{\frac{1}{2}} = c_{-1}\mathbf{b}^1 + (c_0 + c_1)\mathbf{b}^0. \end{array} \tag{7}$$

Constants c_{-1}, c_0 and c_1 can be selected by forcing that these approximations are exact for both constant and linear functions (yielding a second order approximation). This gives the constraints

$$\begin{array}{l} c_{-1} + c_0 + c_1 = 1 \\ c_{-1} - c_1 = \frac{1}{2}. \end{array} \tag{8}$$

For the sake of notation, in the sequel we set $\omega = c_{-1} - c_1$ and $\theta = c_{-1} + c_1$. Note that we can force (7) to be exact also for quadratic functions (yielding a third order accuracy of the approximation (7) with $c_0 = 3/4$, $c_1 = 3/8$ and $c_{-1} = -1/8$), however this does not improve the overall accuracy of the scheme, as we prove in the next subsection. Therefore, θ will be selected on the basis of stability or efficiency constraints.

3 Analysis of the methods

3.1 Consistency

If $\mathbf{a}$ and $\mathbf{b}$ are sufficiently regular functions, the following local truncation error can be straightforwardly derived from standard Taylor expansions:

$$(\mathrm{LTE}_1)_i = \frac{1}{h}\big(y_i(t^{n+1}) - y_i^{n+1}\big) = \left(\frac{1}{2} - \omega\right)\big(\mathtt{a}_i'(t^n)y_i(t^n) - \mathtt{b}_i'(t^n)\big)h + o(h), \tag{9}$$

for $i = 1, \dots, m$. In particular, for $\omega = \frac{1}{2}$ we have:

$$(\mathrm{LTE}_2)_i = \left(\frac{1}{6} - \frac{\theta}{2}\right)\big(\mathtt{a}_i''(t^n)y_i(t^n) - \mathtt{b}_i''(t^n)\big)h^2 + \frac{1}{12}\big(\mathtt{a}_i'(t^n)\mathtt{b}_i^n - \mathtt{a}_i^n\mathtt{b}_i'(t^n)\big)h^2 + o(h^2), \tag{10}$$

	c_{-1}	c_0	c_1
FE*	0	1	0
AB2*	0	$\frac{3}{2}$	-$\frac{1}{2}$
CN*	$\frac{1}{2}$	$\frac{1}{2}$	0
AM3*	$\frac{5}{12}$	$\frac{8}{12}$	$-\frac{1}{12}$
M*(θ)	$\frac{\theta}{2}+\frac{1}{4}$	$1-\theta$	$\frac{\theta}{2}-\frac{1}{4}$

Table 1: Coefficients of the numerical schemes

for $i = 1, \ldots, m$. This implies that the methods are consistent and the LTE features a second order dependence on h independently on θ.

If (8) are fulfilled, we have

$$c_{-1} = \frac{\theta}{2} + \frac{1}{4}, \qquad c_0 = 1 - \theta \quad \text{and} \qquad c_1 = \frac{\theta}{2} - \frac{1}{4}. \tag{11}$$

In the sequel, we adopt this notation that put in evidence the parameter θ.

Notice that the proposed schemes reduce to classical two-steps Adams schemes when $\mathbf{a} = \mathbf{0}$. As a matter of fact, in this case the scheme reduces to

$$y_i^{n+1} = y_i^n + h\left(\left(\frac{\theta}{2}+\frac{1}{4}\right)\mathtt{b}_i^{n+1} + \left(1-\theta\right)\mathtt{b}_i^n + \left(\frac{\theta}{2}-\frac{1}{4}\right)\mathtt{b}_i^{n-1}\right), \quad n = 0, \ldots, N,$$

for $i = 1, \ldots, m,$. We denote these schemes M(θ) and their generalization to the case $\mathbf{a} \neq \mathbf{0}$ M*(θ). Observe, in particular, that M($-\frac{1}{2}$), M($\frac{1}{2}$) and M($\frac{1}{3}$) correponds to the classical Adams-Bashforth two steps scheme (hereafter denoted by AB2), the Crank-Nicolson scheme (CN) and the Adams Moulton two steps scheme (AM3). By extension, we will denote AB2*, CN* and AM3* methods M*($-\frac{1}{2}$), M*($\frac{1}{2}$), M*($\frac{1}{3}$) respectively. We also use the short notation FE* for the Rush-Larsen scheme ($c_{-1} = 0$, $c_0 = 1$ and $c_1 = 0$). In Table 1 we report the coefficients for the numerical schemes used in this paper.

3.2 Stability and Convergence

The numerical method at hand is not a standard multistep or Runge-Kutta method, so we cannot advocate available convergence results and the analysis of the method needs to be explicitly addressed. We give first a definition of zero-stability suitable for our scheme.

Definition 3.1 *A numerical method in the form (6) is zero-stable when*

$$\exists h_0 > 0,\ \exists C > 0 : \forall h \in (0, h_0], \quad \|\mathbf{z}^n - \mathbf{y}^n\| \leq C\varepsilon \quad 0 \leq n \leq N$$

with $\mathbf{y}^n$ *being the solution of problem (6) and* $\mathbf{z}^n$ *being the solution of the perturbed problem*

$$\begin{cases} z_i^{n+1} = z_i^n + h\Phi(\mathtt{a}_i h)\left[\mathtt{a}_i^{n+\frac{1}{2}} z_i^n + \mathtt{b}_i^{n+\frac{1}{2}}\right] + h\delta_i^{n+1} \quad i = 1, \dots, m \\ \mathbf{z}^0 = \mathbf{y}^0 + \delta^0; \end{cases} \tag{12}$$

for $0 \leq n \leq N-1$, *under the assumption that* $\|\delta^k\| \leq \varepsilon$, $0 \leq k \leq N-1$.

Proposition 3.1 *The scheme (6) is zero-stable provided that:*

i) $\mathbf{a}$ *and* $\mathbf{b}$ *are Lipschitz-continuous functions with respect to the first argument and uniformly in time, with constants* L_a *and* L_b *respectively.*

ii) there exists a non-negative constant a_M *such that* $\mathtt{a}_i(\mathbf{y}, t) \leq a_M$, $\forall \mathbf{y} \in \mathbb{R}^m$, $t \in [0, T]$, $i = 1, \dots, m$;

Typically, in gating variable models, $\mathbf{a}_i < 0$, hence condition *ii* holds. This is true, in particular, in the case of Luo Rudy model.
Before proving the Proposition 3.1 we state the following Lemma:

Lemma 3.1 *Let* x^n *satisfies:*

$$0 \leq x^n \leq \xi x^{n-1} + \eta x^{n-2} + (\xi + \eta - 1)\delta, \tag{13}$$

being η, δ, x^0 *and* $x^1 \geq 0$ *and* $\xi \geq 1$. *Then,*

$$x^n \leq \left[x^0 + \delta + \frac{2}{\xi}(x^1 + \delta)\right](\xi + \eta)^n .$$

Proof: We consider the problem:

$$\tilde{x}^n = \xi \tilde{x}^{n-1} + \eta \tilde{x}^{n-2} + (\xi + \eta - 1)\delta, \tag{14}$$

with $\tilde{x}^0 = x^0$ and $\tilde{x}^1 = x^1$. First of all, observe that the right hand side is non-negative, so that assumption (13) makes sense. We have obviously that $x^n \leq \tilde{x}^n$. Solution to difference equation (14) reads

$$\tilde{x}^n = \sigma_1 \rho_1^n + \sigma_2 \rho_2^n - \delta,$$

with

$$\rho_{1,2} = \tfrac{1}{2}\left(\xi \pm \sqrt{\xi^2 + 4\eta}\right), \quad \sigma_1 = \tfrac{(x^1+\delta) - \rho_2(x^0+\delta)}{\rho_1 - \rho_2} \quad \text{and} \quad \sigma_2 = \tfrac{\rho_1(x^0+\delta) - (x^1+\delta)}{\rho_1 - \rho_2}.$$

We notice that $|\rho_{1,2}| \leq \xi + \frac{1}{2}\eta \leq \xi + \eta$ and $|\rho_1 - \rho_2| \geq \xi$; then we can write:

$$x^n \leq \tilde{x}^n \leq \sigma_1 \rho_1^n + |\sigma_2||\rho_2|^n \leq (\sigma_1 + |\sigma_2|)(\xi + \eta)^n ,$$

where we have exploited the fact that $\sigma_1 > 0$. The thesis follows.

Proof of Proposition 3.1 We refer to $||\cdot||_\infty$ (still denoted by $||\cdot||$). We define $(\mathbf{E}(\mathbf{x}))_{ij} = e^{x_i}\delta_{ij}$ where δ_{ij} is the Kronecker symbol, and $(\mathbf{\Phi}(\mathbf{x}))_{ij} = \Phi(x_i)\delta_{ij}$, then, we can rewrite (6) as

$$\mathbf{y}^{n+1} = \mathbf{E}(\mathbf{a}^{n+\frac{1}{2}}h)\,\mathbf{y}^n + \mathbf{\Phi}(\mathbf{a}^{n+\frac{1}{2}}h)\,\mathbf{b}, \quad n = 0, \dots N. \tag{15}$$

We observe that for all $\mathbf{a}$, $\tilde{\mathbf{a}}$ such that $\mathtt{a}_i \le a_M$, and $\tilde{\mathtt{a}}_i \le a_M$ for $i = 1, \dots m$, and $h \in (0, h_0]$ we have:

$$\begin{array}{ll} \|\mathbf{\Phi}(\mathbf{a}h)\| \le \Phi_M, & \|\mathbf{\Phi}(\mathbf{a}h) - \mathbf{\Phi}(\tilde{\mathbf{a}}h)\| \le hL_\Phi\|\mathbf{a} - \tilde{\mathbf{a}}\|, \\ \|\mathbf{E}(\mathbf{a}h)\| \le e^{a_M h}, & \|\mathbf{E}(\mathbf{a}h) - \mathbf{E}(\tilde{\mathbf{a}}h)\| \le hL_e\|\mathbf{a} - \tilde{\mathbf{a}}\|, \end{array} \tag{16}$$

where $\Phi_M = \Phi(a_M h_0)$, $L_\Phi = \Phi'(a_M h_0)$ and $L_e = e^{a_M h_0}$. For the sake of clarity we write $\mathbf{a}_y^n$ and $\mathbf{b}_y^n$ for $\mathbf{a}(\mathbf{y}^n, t^n)$ and $\mathbf{b}(\mathbf{y}^n, t^n)$, and $\mathbf{a}_z^n$ and $\mathbf{b}_z^n$ for $\mathbf{a}(\mathbf{z}^n, t^n)$ and $\mathbf{b}(\mathbf{z}^n, t^n)$. Firstly, we prove that $\mathbf{y}^n$ and $\mathbf{b}_y^n$ are bounded for all $n = 1, \dots, N$. From equation (15) we have

$$\|\mathbf{y}^n\| \le e^{a_M h}\|\mathbf{y}^{n-1}\| + h\Phi_M\|\mathbf{b}_y^{n-\frac{1}{2}}\|, \quad n = 2, \dots, N. \tag{17}$$

Notice that $\|\mathbf{b}(\mathbf{y}, t)\| \le B_0 + L_b\|\mathbf{y}\|$ for all $t \in [0,\, T]$, being $B_0 = \max\limits_{t\in[0,\,T]} \|\mathbf{b}(\mathbf{0}, t)\|$. Hence, we can write:

$$\|\mathbf{b}_y^{n-\frac{1}{2}}\| \le \sum_{k=-1}^{1} \|c_k\mathbf{b}_y^{n-k-1}\| \le \sum_{k=-1}^{1} |c_k B_0| + L_b \sum_{k=-1}^{1} |c_k|\,\|\mathbf{y}^{n-k-1}\| \quad n = 2, \dots, N. \tag{18}$$

Substituting (18) in (17) we have:

$$\alpha\|\mathbf{y}^n\| \le \beta\|\mathbf{y}^{n-1}\| + \gamma\|\mathbf{y}^{n-2}\| + hc\,\Phi_M B_0, \quad n = 2, \dots, N, \tag{19}$$

where $\alpha = 1 - h|c_{-1}|L_b\Phi_M$, $\beta = e^{h\,a_M} + h|c_0|L_b\Phi_M$, $\gamma = h|c_1|L_b\Phi_M$ and $c = |c_{-1}| + |c_0| + |c_1|$. Taking h_0 such that $\alpha > 0 \quad \forall h \in (0, h_0]$, we can apply Lemma 3.1 and obtain, for $n = 2, \dots, N$, the following inequality:

$$\|y^n\| \le \left(\|y^0\| + 2\frac{\alpha}{\beta}\|y^1\| + \left(1 + 2\frac{\alpha}{\beta}\right)\frac{B_0}{L_b}\right)\left(\frac{e^{h\,a_M} + h(|c_0| + |c_1|)L_b\Phi_M}{1 - h|c_{-1}|L_b\Phi_M}\right)^n.$$

Exploiting the well known inequality $(1 + x)^n \le e^{nx}$ for $x \ge 0$, we have:

$$\begin{aligned} \|y^n\| \le \quad & K_1\left(1 + \frac{h|c_{-1}|L_b\Phi_M}{1 - h|c_{-1}|L_b\Phi_M}\right)^n e^{a_M n h}\,(1 + h(|c_0| + |c_1|)L_b\Phi_M)^n \le \\ & K_1\, e^{a_M T} e^{\left(|c_{-1}|(1 - h_0|c_{-1}|L_b\Phi_M)^{-1} + |c_0| + |c_1|\right)L_b\Phi_M T} = y_M, \end{aligned}$$

with $K_1 = \left(\|y^0\| + 2\frac{\alpha}{\beta}\|y^1\| + \left(1 + 2\frac{\alpha}{\beta}\right)\frac{B_0}{L_b}\right)$. Since $\alpha\|y^1\| \le (\beta + \gamma)\|y^0\| + c\,h_0\Phi_M B_0$ we can conclude that y^n is bounded.
Also $\mathbf{b}_y^n$ is bounded $\forall n \in [0, N]$ since $\|\mathbf{b}_y^n\| \le B_0 + L_b y_M = b_M$.

Setting now $\mathbf{w}^n = \mathbf{z}^n - \mathbf{y}^n$ and subtracting (12) from (6) we obtain:

$$\mathbf{w}^n = h\delta^n + \mathbf{E}(h\mathbf{a}_z^{n-\frac{1}{2}})\mathbf{z}^{n-1} - \mathbf{E}(h\mathbf{a}_y^{n-\frac{1}{2}})\mathbf{y}^{n-1} + h\mathbf{\Phi}(h\mathbf{a}_z^{n-\frac{1}{2}})\mathbf{b}_z^{n-\frac{1}{2}} - h\mathbf{\Phi}(h\mathbf{a}_y^{n-\frac{1}{2}})\mathbf{b}_y^{n-\frac{1}{2}}, \tag{20}$$

for $n = 1, \ldots, N$. Let us analyze separately the terms of the previous equation.

$$\begin{aligned}
&\left\| \mathbf{E}(h\mathbf{a}_z^{n-\frac{1}{2}})\mathbf{z}^{n-1} - \mathbf{E}(h\mathbf{a}_y^{n-\frac{1}{2}})\mathbf{y}^{n-1} \right\| = \\
&\quad \left\| \mathbf{E}(h\mathbf{a}_z^{n-\frac{1}{2}})\mathbf{w}^{n-1} + \left(\mathbf{E}(h\mathbf{a}_z^{n-\frac{1}{2}}) - \mathbf{E}(h\mathbf{a}_y^{n-\frac{1}{2}}) \right) \mathbf{y}^{n-1} \right\| \leq \\
&\quad e^{h\,a_M} \|\mathbf{w}^{n-1}\| + h y_M L_e \left\| \mathbf{a}_z^{n-\frac{1}{2}} - \mathbf{a}_y^{n-\frac{1}{2}} \right\| \leq \\
&\quad e^{h\,a_M} \|\mathbf{w}^{n-1}\| + h y_M L_e L_a \left(\textstyle\sum_{i=-1}^{1} |c_i| \, \|\mathbf{w}^{n-i-1}\| \right);
\end{aligned}$$

$$\begin{aligned}
&\left\| \mathbf{\Phi}(h\mathbf{a}_z^{n-\frac{1}{2}})\, \mathbf{b}_z^{n-\frac{1}{2}} - \mathbf{\Phi}(h\mathbf{a}_y^{n-\frac{1}{2}})\mathbf{b}_y^{n-\frac{1}{2}} \right\| = \\
&\quad \left\| \mathbf{\Phi}(h\mathbf{a}_z^{n-\frac{1}{2}})(\mathbf{b}_z^{n-\frac{1}{2}} - \mathbf{b}_y^{n-\frac{1}{2}}) + (\mathbf{\Phi}(h\mathbf{a}_z^{n-\frac{1}{2}}) - \mathbf{\Phi}(h\mathbf{a}_z^{n-\frac{1}{2}}))\mathbf{b}_y^{n-\frac{1}{2}} \right\| \leq \\
&\quad \Phi_M \left\| \mathbf{b}_z^{n-\frac{1}{2}} - \mathbf{b}_y^{n-\frac{1}{2}} \right\| + b_M L_\Phi \left\| \mathbf{a}_z^{n-\frac{1}{2}} - \mathbf{a}_y^{n-\frac{1}{2}} \right\| \leq \\
&\quad (\Phi_M L_b + h b_M L_\Phi L_a) \left(\textstyle\sum_{i=-1}^{1} |c_i| \, \|\mathbf{w}^{n-i-1}\| \right).
\end{aligned}$$

From equation (20), using previous inequalities, we obtain:

$$\alpha \|\mathbf{w}^n\| \leq \beta \|\mathbf{w}^{n-1}\| + \gamma \|\mathbf{w}^{n-2}\| + h\varepsilon,$$

where $\alpha = 1 - h|c_{-1}|K_2$, $\beta = e^{h\,a_M} + h|c_0|K_2$, $\gamma = h|c_1|K_2$ with $K_2 = (y_M L_e L_a + \Phi_M L_b + h_0 b_m L_\Phi L_a)$. If we take h_0 such that $\alpha > 0 \forall h \in (0, h_0]$, we can apply Lemma 3.1 and obtain:

$$\|\mathbf{w}^n\| \leq \left(\|\mathbf{w}^0\| + 2\frac{\alpha}{\beta}\|\mathbf{w}^1\| + \left(1 + 2\frac{\alpha}{\beta}\right) \frac{\varepsilon}{cK_2} \right) \left(\frac{e^{h\,a_M} + h(|c_0| + |c_1|)K_2}{1 - h|c_{-1}|K_2} \right)^n,$$

for $n = 2, \ldots, N$. Noticing that $\|\mathbf{w}^0\| \leq \varepsilon$, $\alpha|\mathbf{w}^1| \leq (\beta + \gamma)|\mathbf{w}^0| + h_0\varepsilon$ and that $(1 + x)^n \leq e^{nx}$ for $x \geq 0$ we obtain, for $n = 1, \ldots, N$:

$$\begin{aligned}
\|\mathbf{w}^n\| &\leq \varepsilon \left(3 + 2\frac{\gamma}{\beta} + \frac{\beta + 2\alpha}{\beta c K_2} \right) \left(1 + \frac{h|c_{-1}|K_2}{1 - h|c_{-1}|K_2} \right)^n e^{a_M n h}\, e^{(|c_0| + |c_1|)K_2 n h} \leq \\
&\quad \varepsilon \left(3 + 2\frac{\gamma}{\beta} + \frac{\beta + 2\alpha}{\beta c K_2} \right) e^{a_M T} e^{\left(|c_{-1}|(1 - h_0|c_{-1}|C)^{-1} + |c_0| + |c_1| \right) C T},
\end{aligned}$$

which proves the thesis.

Should $\mathbf{a}(t, \mathbf{y})$ and $\mathbf{b}(t, \mathbf{y})$ be sufficiently regular functions, zero-stability and consistency allow to conclude that the method is convergent with order 2 if $\omega = 1/2$ and order 1 otherwise.

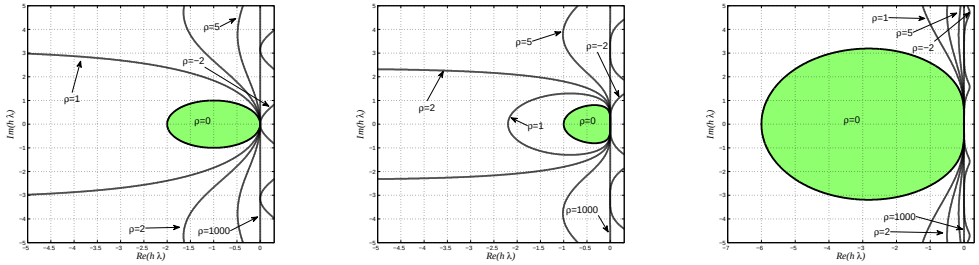

Figure 2: Absolute stability regions for the FE* (left), the AB2* (center) and AM3* methods on the model problem $y' = \lambda y$ with $\lambda = \lambda_a + \lambda_b$ $\mathtt{a} = \lambda_a$, $\mathtt{b} = \lambda_b y$ and $\lambda_a = \rho\lambda_b$ with ρ a real parameter.

3.3 Absolute stability

The stability over long time intervals for the model linear problem $y = \lambda y$, with $Re(\lambda) < 0$ strongly depends on the implementation of the method, i.e. on the definition on $\mathtt{a}$ and $\mathtt{b}$ with respect to the model problem. In particular, since the part driven by $\mathtt{a}$ is solved exactly for the model problem, if we set $\mathtt{a} = \lambda$ ($\mathtt{b} = 0$) we get an unconditionally stable method, whilst for $\mathtt{a} = 0$ and $\mathtt{b} = \lambda y$ stability of the method is the one of the correspondent multistep method. These preliminary observations match with the experimental results mentioned above, concerning the FE* method which is more stable than the corresponding FE scheme. In order to be more quantitative, we split $\lambda = \lambda_a + \lambda_b$ and consider the (scalar) scheme (6) with $\mathtt{a} = \lambda_a$ and $\mathtt{b} = \lambda_b$. In particular, we write $\lambda_a = \rho\lambda_b$ where ρ is a non-negative parameter, and investigate the time asymptotic solution dynamics for different values of ρ and different schemes.

By standard arguments on finite difference equations, we obtain that the solution computed by our scheme asymptotically vanishes if the roots of the polynomial

$$\left(1 - \frac{e^{\frac{\rho\lambda h}{\rho+1}} - 1}{\rho} c_{-1}\right) r^2 - \left(1 + \left(e^{\frac{\rho\lambda h}{\rho+1}} - 1\right)\left(1 + \frac{c_0}{\rho}\right)\right) r - c_1 \frac{e^{\frac{\rho\lambda h}{\rho+1}} - 1}{\rho} = 0$$

belong to the unit circle in the complex plane. We stress that for $\rho \to 0$ we recover the characteristic polynomial of the method $\mathrm{M}(\theta)$. In Fig. 2 we report the region of absolute stability of FE2*, AB2* and AM3* respectively. The shaded region is the region of absolute stability of the corresponding traditional multistep method. As expected, when ρ gets larger, the region of absolute stability increases and the method at hand tends to become unconditionally stable (and exact for the model problem).

This analysis gives an interesting perspective to the methods addressed here, that can be considered a sort of "stabilization" of traditional schemes, which is

however obtained by limiting the accuracy to the second order.

Observe that for $\rho < -1$ we have $\lambda_a < 0$ and $\lambda_b > 0$ that is the situation we have from the linearization of problems coming from electro-physiology. In this case, the region of absolute stability covers the entire half plane.

3.4 Positivity properties

As pointed out previously, one of the interesting features of the Rush-Larsen scheme, solving the gating equations, is that the numerical solution belongs to the interval [0, 1]. Here, we investigate the positivity properties of our schemes, giving a rigorous proof that holds also for the Rush-Larsen scheme itself. Let us start with some assumptions on the continuous problems, that are in particular verified for the applications of interest here.

Let us suppose that there exist a function $\mathtt{a}(t, y) < 0$ and constants K_1, K_2 such that:

$$\mathtt{a}(t, y)(y - K_1) \leq f(t, y) \leq \mathtt{a}(t, y)(y - K_2) \quad \forall y \in \mathbb{R},\, t \in (0, T] \tag{21}$$

then the solution $y \in [K_1, K_2]$ provided that $y^0 \in [K_1, K_2]$ (in the case of gating variables $K_1 = 0$ and $K_2 = 1$). This can be proved considering the subsolution $\underline{y}$ and the supersolution $\overline{y}$ fulfilling the equations:

$$\begin{cases} \dfrac{d\underline{y}}{dt} = \mathtt{a}(t, \underline{y})(\underline{y} - K_1) \\ \underline{y}(0) = y_0 \end{cases} \qquad \begin{cases} \dfrac{d\overline{y}}{dt} = \mathtt{a}(t, \overline{y})(\overline{y} - K_2) \\ \overline{y}(0) = y_0. \end{cases} \tag{22}$$

We have that $\underline{y} \leq y \leq \overline{y}$. We claim that $\underline{y} \geq K_1$. In fact, multiplying the first equation in (22) by $(\underline{y} - K_1)$, we get

$$\frac{1}{2}\frac{d}{dt}(\underline{y} - K_1)^2 = \mathtt{a}(\underline{y} - K_1)^2 \leq 0.$$

Hence, since $(\underline{y} - K_1)^2$ is decreasing in time, if there exists $\tau \in [0, T]$ such that $\underline{y}(\tau) = K_1$, then $\underline{y}(t) = K_1$ for all $t \in [\tau, T]$. With same arguments we conclude that $\overline{y}(t) \leq K_2$. Hence $K_1 \leq \underline{y} \leq y \leq \overline{y} \leq K_2$.

Setting $\mathtt{b}(t, y) = f(t, y) - \mathtt{a}(t, y)y$, the problem can be solved using the proposed schemes that, for the sake of clarity, we write as

$$y^{n+1} = e^{\mathtt{a}^{n+\frac{1}{2}}h} y^n + \left(1 - e^{\mathtt{a}^{n+\frac{1}{2}}h}\right)\left(-\frac{\mathtt{b}^{n+\frac{1}{2}}}{\mathtt{a}^{n+\frac{1}{2}}}\right).$$

We start assuming that $\mathtt{a}^{n+\frac{1}{2}}$ and $\mathtt{b}^{n+\frac{1}{2}}$ are exactly $\mathtt{a}(t^{n+\frac{1}{2}})$ and $\mathtt{b}(t^{n+\frac{1}{2}})$. If $y^n \in [K_1, K_2]$, under the assumption (21), y^{n+1} is the convex combination (with coefficients $e^{\mathtt{a}^{n+\frac{1}{2}}h}$ and $1 - e^{\mathtt{a}^{n+\frac{1}{2}}h}$) of terms ($y^n$ and $\dfrac{\mathtt{a}^{n+\frac{1}{2}}}{\mathtt{b}^{n+\frac{1}{2}}}$) belonging to

the range $[K_1, K_2]$. Hence y^{n+1} belongs to the same range. With induction arguments, we conclude that y^n belongs to $[K_1, K_2]$ when y^0 does.

Now, we have to investigate the impact of the approximations $\mathtt{a}^{n+\frac{1}{2}} \simeq \mathtt{a}(t^{n+\frac{1}{2}})$ and $\mathtt{b}^{n+\frac{1}{2}} \simeq \mathtt{b}(t^{n+\frac{1}{2}})$ on this statement. If the three coefficients c_{-1}, c_0, c_1 are non negative, then the combination still features positive coefficients and $-\frac{\mathtt{b}^{n+1}}{\mathtt{a}^{n+1}}$ is in the range $[K_1, K_2]$. Therefore, we have proved the following proposition:

Proposition 3.2 *Under the assumption (21), the schemes (6) with non-negative coefficients c_{-1}, c_0 and c_1, have numerical solution $y^n \in [K_1, K_2]$, provided that $y^0 \in [K_1, K_2]$.*

Notice that the latter proposition includes the schemes FE*, CN* and M$(\theta)^*$ with $\theta > 0$.

A special consideration deserves the explicit second order scheme AB2*.

Proposition 3.3 *Let $f(t, y)$ fulfills inequalities (21) with $\mathtt{a}$ constant, $y^0 \in [K^1, K^2]$ and define $\mathtt{b} := f - \mathtt{a}y$. Then the scheme AB2* is such that the numerical solution y^n belongs to $[K^1, K^2]$ when*

$$h \leq \frac{\log(2)}{|\mathtt{a}|}. \tag{23}$$

Moreover, if the initial conditions are such that

$$\left(\frac{3}{2}e^{\mathtt{a}h} - \frac{1}{2}\right) K_1 \leq e^{\mathtt{a}h} y^1 - h\Phi\frac{1}{2}\mathtt{b}^0 \leq \left(\frac{3}{2}e^{\mathtt{a}h} - \frac{1}{2}\right) K_2 \tag{24}$$

we can relax the restriction on h and ask that

$$h \leq \frac{\log(3)}{|\mathtt{a}|}. \tag{25}$$

The restrictions on h (23) and (25) are to be compared with the ones of AB2 [10], namely $h \leq \frac{1}{3|\mathtt{a}|}$ and $h \leq \frac{4}{9|\mathtt{a}|}$ respectively. Hence, AB2* allows us to take significantly higher values than what AB2 does.

Proof Firstly, we notice that y^n fulfills the scheme (2), then $u^n := y^n - K^1$ satisfies the scheme $u^{n+1} = u^n + h\Phi(\mathtt{a}h)(\mathtt{a}u^n + \tilde{\mathtt{b}}^{n+\frac{1}{2}})$, being $\tilde{\mathtt{b}}^{n+\frac{1}{2}} := \frac{3}{2}\tilde{\mathtt{b}}^n - \frac{1}{2}\tilde{\mathtt{b}}^{n-1}$ and $\tilde{\mathtt{b}}^n := \mathtt{b}^n + \mathtt{a}K^1$. In fact:

$$\begin{aligned} &u^{n+1} = y^{n+1} - K^1 = y^n + h\Phi(\mathtt{a}h)\left(\mathtt{a}y^n + b^{n+\frac{1}{2}}\right) - K^1 = \\ &y^n - K^1 + h\Phi(\mathtt{a}h)\left(\mathtt{a}(y^n - K^1) + (b^{n+\frac{1}{2}} + \mathtt{a}K^1)\right) = \\ &u^n + h\Phi(\mathtt{a}h)\left(\mathtt{a}u^n + \tilde{\mathtt{b}}^{n+\frac{1}{2}}\right). \end{aligned} \tag{26}$$

We notice that (21) implies $\tilde{b}^n \geq 0$. Analogously, $u^n := K^2 - y^n$ satisfies the same scheme, with $\tilde{\mathtt{b}}^n := -\mathtt{b}^n - \mathtt{a}K^2$ and $\tilde{\mathtt{b}}^n \geq 0$; hence, by proving that $u^n \geq 0$

we prove that $y^n \in [K^1, K^2]$. We prove that $u^n \geq 0$ by induction. Let us define $s^n = e^{\mathtt{a}h}u^n - h\Phi(\mathtt{a}h)\frac{1}{2}\tilde{\mathtt{b}}^{n-1}$, we have

1. $s^1 \geq 0$. In fact,
$$s^1 = e^{\mathtt{a}h}u^1 - h\Phi(\mathtt{a}h)\frac{1}{2}\tilde{\mathtt{b}}^0$$
which is non negative when (24) holds; otherwise, since $u^1 = e^{\mathtt{a}h}u^0 + h\Phi(\mathtt{a}h)\tilde{\mathtt{b}}^0$, s^1 can be written as
$$s^1 = e^{2\mathtt{a}h}u^0 + h\Phi(\mathtt{a}h)\left(e^{\mathtt{a}h} - \frac{1}{2}\right)\tilde{\mathtt{b}}^0,$$
which is non negative when $\left(e^{\mathtt{a}h} - \frac{1}{2}\right) \geq 0$, i.e. when (23) holds.

2. $s^n \geq 0 \implies s^{n+1} \geq 0$, $n = 1, \ldots, N-1$.
In fact, $u^{n+1} = e^{\mathtt{a}h}u^n + h\Phi(\mathtt{a}h)\left(\frac{3}{2}\tilde{\mathtt{b}}^n - \frac{1}{2}\tilde{\mathtt{b}}^{n-1}\right)$, hence
$$\begin{aligned}
&s^{n+1} = e^{\mathtt{a}h}u^{n+1} - h\Phi(\mathtt{a}h)\frac{1}{2}\tilde{\mathtt{b}}^n = \\
&e^{\mathtt{a}h}\left[e^{\mathtt{a}h}u^n + h\Phi(\mathtt{a}h)\left(\frac{3}{2}\tilde{\mathtt{b}}^n - \frac{1}{2}\tilde{\mathtt{b}}^{n-1}\right)\right] - h\Phi(\mathtt{a}h)\frac{1}{2}\tilde{\mathtt{b}}^n = \\
&e^{\mathtt{a}h}\left[e^{\mathtt{a}h}u^n - h\Phi(\mathtt{a}h)\frac{1}{2}\tilde{\mathtt{b}}^{n-1}\right] + h\Phi(\mathtt{a}h)\left(\frac{3}{2}e^{\mathtt{a}h} - \frac{1}{2}\right)\tilde{\mathtt{b}}^n \geq \\
&e^{\mathtt{a}h}s^n + h\Phi(\mathtt{a}h)\left(\frac{3}{2}e^{\mathtt{a}h} - \frac{1}{2}\right)\tilde{\mathtt{b}}^n \geq h\Phi(\mathtt{a}h)\left(\frac{3}{2}e^{\mathtt{a}h} - \frac{1}{2}\right)\tilde{\mathtt{b}}^n.
\end{aligned} \tag{27}$$
The last term is non negative when $\left(\frac{3}{2}e^{\mathtt{a}h} - \frac{1}{2}\right) \geq 0$, i.e. when (25) holds (notice that $s^n \geq 0 \implies u^n \geq 0$, since $e^{\mathtt{a}h}u^n \geq +h\Phi(\mathtt{a}h)\frac{1}{2}\tilde{\mathtt{b}}^{n-1} \geq 0$; for this reason $\tilde{b}^n \geq 0$).

Hence, by induction, $s^n \geq 0, n = 1, \ldots, N$. This implies $u^n \geq 0$.

4 The scheme at work

In this section we show how to use the proposed scheme for the solution of system (1). In scheme (6) we take $\mathbf{a} = [0, \boldsymbol{a}^T, \mathbf{0}^T]^T$ and $\mathbf{b} = [I, \boldsymbol{b}^T, \mathbf{g}^T]^T$, hence, the scheme reads as follows:

$$\begin{cases}
\frac{1}{h}u^{n+1} = \frac{1}{h}u^n + c_{-1}\, I^{n+1} + c_0\, I^n + c_1\, I^{n-1} \\
\frac{1}{h}w_i^{n+1} = \frac{1}{h}w_i^n + \Phi(a_i^{n+\frac{1}{2}}h)\left(a_i^{n+\frac{1}{2}}w_i^n + b_i^{n+\frac{1}{2}}\right) \quad i = 1, \ldots, m \\
\frac{1}{h}\mathbf{X}^{n+1} = \frac{1}{h}\mathbf{X}^n + c_{-1}\, \mathbf{g}^{n+1} + c_0\, \mathbf{g}^n + c_1\, \mathbf{g}^{n-1} \\
u(0) = u_0, \quad \mathbf{w}(0) = \mathbf{w}_0, \quad \mathbf{X}(0) = \mathbf{X}_0,
\end{cases} \tag{28}$$

for $n = 0, \ldots, N$. We take $I^{-1} = I^0$ and $\mathbf{g}^{-1} = \mathbf{g}^0$. The following results are obtained using the Luo-Rudy phase I model with the following current stimulus:

$$I_{app} = \begin{cases} I_{max}\left(\frac{1}{2} - \frac{1}{2}\cos\left(2\pi\frac{t}{t_p}\right)\right) & t < t_p \\ 0 & t \geq t_p, \end{cases} \qquad I_{max} = 60\mu A, \quad t_p = 1ms, \tag{29}$$

and $C_m = 1\mu\ F$. We refer to the discrete L^2 norm of the components of solution y^n, defined as

$$\|y_i\| = \sqrt{\frac{1}{2}\sum_{n=0}^{N-1}\left[(y_i^n)^2 + \left(y_i^{n+1}\right)^2\right](t^{n+1} - t^n)}.$$

The relative error is computed as $\max_i \dfrac{\|y_i(t^n) - y_i^n\|}{\|y_i(t^n)\|}$. In the following simulations we will take $T = 450\ ms$. In Table 2 we compare the relative errors for different time steps using our explicit method AB2*, FE*, and their corresponding multistep methods, AB2 and FE. The reference solution is obtained solving the system with the Matlab function `ode45` with parameters `RelTol` and `AbsTol` set respectively to $1e-9$ and $1e-12$. Results confirm that AB2* method is second order accurate and hence more accurate than the Rush-Larsen method. Observe that for tiny time-steps multistep methods feature slightly better than the correspondent starred methods, and however, their stability constraints are strong, requiring $h \leq 0.1\ ms$.

h	err_{rel} AB2*	err_{rel} FE*	err_{rel} AB2	err_{rel} FE
2e-1	1.03-1	1.02e-1	`NaN`	`NaN`
1e-1	8.73e-3	6.72e-2	`NaN`	`NaN`
5e-2	3.64e-3	3.98e-2	`NaN`	`NaN`
2.5e-2	1.28e-3	2.16e-2	`NaN`	`NaN`
1.25e-2	3.63e-4	1.12e-2	`NaN`	6.65e-3
6.25e-3	9.71e-5	5.65e-3	5.65e-5	3.33e-3

Table 2: Relative error using different time-steps and the methods AB2*, FE*, AB2 and FE.

4.1 Predictor-corrector strategy

Now we want to use our schemes with a predictor-corrector (PC) strategy (for an introduction on predictor-corrector scheme, see [13, 17]). Let $\hat{\mathbf{y}}^n$ be the solution obtained with the (explicit) predictor scheme, and $\mathbf{y}^n$ the one obtained with the (implicit) corrector scheme; let $\overline{c}_0$ and $\overline{c}_1$ be the coefficients of predictor scheme ($\overline{c}_{-1} = 0$) and c_{-1}, c_0, c_1 the coefficients of the corrector scheme. The PC time

h	AB2*-CN*	FE*-CN*	AB2*-CN*$_{PEC}$	FE*-CN*$_{PEC}$
2e-1	3.41-2	5.65e-2	NaN	4.26e-2
1e-1	9.02e-3	2.33e-2	1.50e-2	3.04e-2
5e-2	2.97e-3	7.72e-3	4.15e-3	1.26e-2
2.5e-2	6.95-4	2.23e-3	9.00e-4	3.95e-3
1.25e-2	1.57e-4	6.03e-4	1.85e-4	1.09e-3
6.25e-3	3.77e-5	1.58e-4	4.16e-5	2.88e-4

Table 3: Relative errors using different time-steps and the predictor-corrector methods AB2*-CN*, FE*-CN*. The results in the first two columns refer to the PECE approach, the ones in last two columns to the PEC approach.

discretization of system (1), for $n = 1, \dots, N$, reads:

$$
\begin{aligned}
P:&\begin{cases}
\frac{1}{h}\hat{u}^{n+1} = \frac{1}{h}u^n + \overline{c}_0\, I^n + \overline{c}_1\, I^{n-1} \\
\frac{1}{h}\hat{w}_i^{n+1} = \frac{1}{h}w_i^n + \Phi(\overline{a}_i^{n+\frac{1}{2}}h)\left(\overline{a}_i^{n+\frac{1}{2}} w_i^n + \overline{b}_i^{n+\frac{1}{2}}\right) \quad i = 1, \dots, m \\
\frac{1}{h}\hat{\mathbf{X}}^{n+1} = \frac{1}{h}\mathbf{X}^n + \overline{c}_0\, \mathbf{g}^n + \overline{c}_1\, \mathbf{g}^{n-1}
\end{cases} \\
C:&\begin{cases}
\frac{1}{h}u^{n+1} = \frac{1}{h}u^n + c_{-1}\hat{I}^{n+1} + c_0 I^n + c_1 I^{n-1} \\
\frac{1}{h}w_i^{n+1} = \frac{1}{h}w_i^n + \Phi\big((\hat{a}_i^{n+\frac{1}{2}}h)\left(a_i^{n+\frac{1}{2}}\, w_i^n + \hat{b}_i^{n+\frac{1}{2}}\right) \quad i = 1, \dots, m \\
\frac{1}{h}\mathbf{X}^{n+1} = \frac{1}{h}\mathbf{X}^n + c_{-1}\hat{\mathbf{g}}^{n+1} + c_0\mathbf{g}^n + c_1\, \mathbf{g}^{n-1},
\end{cases}
\end{aligned}
\tag{30}
$$

where $\hat{I}^{n+1}$ and $\hat{\mathbf{g}}^{n+1}$ are computed using the predictor solutions $\hat{u}^{n+1}$, $\hat{\mathbf{w}}^{n+1}$, $\hat{\mathbf{X}}^{n+1}$ and:

$$
\begin{aligned}
&\overline{\boldsymbol{a}}^{n+\frac{1}{2}} = \overline{c}_0\boldsymbol{a}^n + \overline{c}_1\boldsymbol{a}^{n-1}, \quad \overline{\mathbf{b}}^{n+\frac{1}{2}} = \overline{c}_0\mathbf{b}^n + \overline{c}_1\mathbf{b}^{n-1}, \\
&\hat{\boldsymbol{a}}^{n+\frac{1}{2}} = c_{-1}\boldsymbol{a}(\hat{u}^{n+1}) + c_0\boldsymbol{a}^n + c_1\boldsymbol{a}^{n-1}; \quad \hat{\mathbf{b}}^{n+\frac{1}{2}} = c_{-1}\mathbf{b}(\hat{u}^{n+1}) + c_0\mathbf{b}^n + c_1\mathbf{b}^{n-1}. \\
&\overline{\boldsymbol{a}}^{\frac{1}{2}} = (\overline{c}_0 + \overline{c}_1)\boldsymbol{a}^0, \quad \overline{\mathbf{b}}^{\frac{1}{2}} = (\overline{c}_0 + \overline{c}_1)\mathbf{b}^0, \\
&\hat{\boldsymbol{a}}^{\frac{1}{2}} = c_{-1}\boldsymbol{a}(\hat{u}^1) + (c_0 + c_1)\boldsymbol{a}^0, \quad \hat{\mathbf{b}}^{\frac{1}{2}} = c_{-1}\mathbf{b}(\hat{u}^1) + (c_0 + c_1)\mathbf{b}^0.
\end{aligned}
\tag{31}
$$

In Tables 3 and 4 we show relative errors for different predictor-corrector schemes. We note that the best performances are obtained using a second order predictor scheme with a PECE approach (for definition of PECE and PEC approach see [13] or [17]). Also the CN* corrector scheme performs slightly better than the AM3* one. As expected, the differences between PECE approach and PEC are more evident when large time-steps are used.

5 Time adaptive strategy

Using an error estimate based on the PC strategy, we can devise a time-adaptive strategy.

h	AB2*-AM3*	FE*-AM3*	AB2*-AM3*$_{PEC}$	FE*-AM3*$_{PEC}$
2e-1	6.44-2	4.07e-2	NaN	3.94e-2
1e-1	7.84e-3	2.02e-2	1.19e-2	2.91e-2
5e-2	2.67e-3	7.03e-3	3.75e-3	1.26e-2
2.5e-2	6.76e-4	2.07e-3	8.73e-4	4.02e-3
1.25e-2	1.62e-4	5.60e-4	1.91e-4	1.13e-3
6.25e-3	4.13e-5	1.47e-4	4.51e-5	2.98e-4

Table 4: Relative errors using different time-steps and the predictor-corrector methods AB2*-AB3*, FE*-AB3*. The results in the first two columns refer to the PECE approach, while in the last two columns to the PEC approach.

5.1 A posteriori error estimation

We are looking for an estimate of error between $\mathbf{y}(t^{n+1})$ and $\mathbf{y}^{n+1}$ depending on the computed solutions $\mathbf{y}^{n+1}$ and $\hat{\mathbf{y}}^{n+1}$ (for multistep methods this estimate is called Milne's estimate, see [13]). We start considering a predictor-corrector couple of second order schemes, with parameters θ_p and θ_c respectively. From (10) we have, for $i = 1, \ldots, m$,

$$
\begin{aligned}
&y_i(t^{n+1}) - \hat{y}_i^{n+1} = \\
&\quad \left(\tfrac{1}{6} - \tfrac{\theta_p}{2}\right)\left(\mathtt{a}_i''(t^n)y_i(t^n) - \mathtt{b}_i''(t^n)\right)h^3 + \tfrac{1}{12}\left(\mathtt{a}_i'(t^n)\mathtt{b}_i^n - \mathtt{a}_i^n\mathtt{b}_i'(t^n)\right)h^3 + o(h^3); \\
&y_i(t^{n+1}) - y_i^{n+1} = \\
&\quad \left(\tfrac{1}{6} - \tfrac{\theta_c}{2}\right)\left(\mathtt{a}_i''(t^n)y_i(t^n) - \mathtt{b}_i''(t^n)\right)h^3 + \tfrac{1}{12}\left(\mathtt{a}_i'(t^n)\mathtt{b}_i^n - \mathtt{a}_i^n\mathtt{b}_i'(t^n)\right)h^3 + o(h^3).
\end{aligned}
\tag{32}
$$

Subtracting equation $(32)_1$ from $(32)_2$ we have:

$$
\left(\mathtt{a}_i''(t^n)y_i(t^n) - \mathtt{b}_i''(t^n)\right)h^3 = \frac{2}{\theta_c - \theta_p}\left(y_i^{n+1} - \hat{y}_i^{n+1}\right) + o(h^3). \tag{33}
$$

Substituting the latter equation into $(32)_2$, we have:

$$
y_i(t^{n+1}) - y_i^{n+1} = \frac{\theta_c - \frac{1}{3}}{\theta_p - \theta_c}\left(y_i^{n+1} - \hat{y}_i^{n+1}\right) + \tfrac{1}{12}\left(\mathtt{a}_i'(t^n)\mathtt{b}_i^n - \mathtt{a}_i^n\mathtt{b}_i'(t^n)\right)h^3 + o(h^3). \tag{34}
$$

In view of an *a posteriori* error estimator, the first derivatives of $\mathbf{a}$ and $\mathbf{b}$ can be approximated by forward differences,

$$
\mathtt{a}_i'(t^n)\mathtt{b}_i^n - \mathtt{a}_i^n\mathtt{b}_i'(t^n) = \frac{1}{h}\left(\mathtt{a}_i^{n+1}\,\mathtt{b}_i^n - \mathtt{a}_i^n\,\mathtt{b}_i^{n+1}\right) + O(h);
$$

then, we obtain the following error estimate:

$$
y_i(t^{n+1}) - y_i^{n+1} = \frac{\theta_c - \frac{1}{3}}{\theta_p - \theta_c}\left(y_i^{n+1} - \hat{y}_i^{n+1}\right) + \frac{1}{12}\left(\mathtt{a}_i^{n+1}\,\mathtt{b}_i^n - \mathtt{a}_i^n\,\mathtt{b}_i^{n+1}\right)h^2 + o(h^3). \tag{35}
$$

h	AB2*-CN$^*_e$	AB2*-AM3$^*_e$	AB2*-CN$^*_{e-PEC}$	AB2*-AM3$^*_{e-PEC}$
2e-1	NaN	NaN	NaN	NaN
1e-1	8.16e-3	8.06e-3	4.46e-3	4.59e-3
5e-2	3.84e-4	3.91e-4	1.91e-3	1.92e-3
2.5e-2	4.88e-5	4.91e-5	3.48e-4	3.49e-4
1.25e-2	7.03e-6	7.03e-6	4.97e-5	4.97e-5
6.25e-3	4.35e-6	4.35e-6	9.48e-6	9.48e-5

Table 5: Relative error using different time-steps and the predictor-corrector methods AB2*-AB3*, FE*-AB3* corrected with local extrapolation. The results in the first two columns refer to the PECE approach, while in the last two columns to the PEC approach.

For first order predictor-corrector couples, with parameters ω_p and ω_c respectively (and $\neq 1/2$), we get the following error estimate:

$$\mathbf{y}(t^{n+1}) - \mathbf{y}^{n+1} = \frac{\omega_c - \frac{1}{2}}{\omega_p - \omega_c} \left(\mathbf{y}^{n+1} - \hat{\mathbf{y}}^{n+1}\right) + o(h^2). \tag{36}$$

In principle, these estimates can be used to improve the solution so to get a third order method (*local extrapolation*). As a matter of fact, once computed the error estimate $\mathbf{E}^{n+1}$, we compute $\tilde{\mathbf{y}}^{n+1} = \mathbf{y}^{n+1} + \mathbf{E}^{n+1}$, raising by one the order of the method. In Table 5 we show relative errors of predictor-corrector schemes corrected with this *a posteriori* error estimation. We observe very slight differences between the schemes, the PECE approach performing better than the PEC approach. These schemes are more accurate than the second order one (compare Table 5 with Tables 3 and 4), however we notice that for large time-steps they become unstable. Moreover, using this local extrapolation, we loose the favourable positivity properties of the non corrected schemes.

5.2 Time adaptive schemes

Given a vector of tolerances $\boldsymbol{\tau}$ (possibly a different tolerance for each variable), we look for the largest time-step such that $E_i^n \leq \tau_i$, $i = 1, \ldots, m$. Using a first order method $E_i^n \simeq K_i h^2$, being $\mathbf{K}$ a constant vector, if $\mathbf{E}^n$ is the error obtained with a time-step h, then using a time-step $\tilde{h} = \min_i h\sqrt{\frac{E_i^n}{\tau_i}}$ we can obtain an error $\tilde{\mathbf{E}}$ such that $\tilde{E}_i^n \simeq \tau_i$ for some i. Using a second order method the optimal time-step is given by $\tilde{h} = \min_i h\sqrt[3]{\frac{E_i^n}{\tau_i}}$, (see [13]). Sometimes the vector of tolerances is defined as $\boldsymbol{\tau} = \max(\boldsymbol{\tau}_{abs} + \tau_{rel}\mathbf{y})$, being $\boldsymbol{\tau}_{abs}$ and τ_{rel} respectively a vector of absolute tolerances and a relative tolerance. This is, for example, the choice of Matlab for `odexx` suite. In our simulations, however, we weighted the tolerances based on the infinity norm of the components of the solution, hence, for the

Luo-Rudy model from Figure 1 we get $\boldsymbol{\tau} = \tau\,[84,\ 1,\ 1,\ 1,\ 1,\ 1,\ 1,\ 7e-3]^T$. The time adapting algorithm reads therefore While $t^n < T$

1. Compute $\hat{\mathbf{y}}^{n+1}$ and $\mathbf{y}^{n+1}$ with time-step h
2. Compute the error $\mathbf{E}^{n+1}$
3. If $E_i^{n+1} < \tau_i$ then $t^{n+1} = t^n + h$, $n = n+1$
4. Compute $\tilde{h}$, set $h = 0.95\,\tilde{h}$ (0.95 is a cautelative parameter).

We define the recomputed percentage r as the percentage of the number of times the conditional expression 3 is false over the total number of steps n.
In order to deal with variable time-steps we have to change the schemes coefficients. In particular, if $\nu = \frac{h}{h_{old}}$ is the ratio between the time-step at the current iteration and the time-step at the previous iteration, we take $\tilde{c}_{-1} = c_{-1}$, $c_0 = c_0 + c_1(1-\nu)$ and $\tilde{c}_1 = \nu c_1$ as the coefficient of the variable step scheme. Writing the Taylor expansions of $a^{n+\frac{1}{2}}$ and $b^{n+\frac{1}{2}}$ and taking in account that $t^{n+1} - t^n = h$ and $t^n - t^{n-1} = \frac{h}{\nu}$, we obtain:

$$\begin{aligned} \mathbf{a}^{n+\frac{1}{2}} &= \mathbf{a}^n + \tilde{\omega}\mathbf{a}'(t_n)h + \tilde{\theta}\mathbf{a}''(t_n)\tfrac{h^2}{2} + o(h^2); \\ \mathbf{b}^{n+\frac{1}{2}} &= \mathbf{b}^n + \tilde{\omega}\mathbf{b}'(t_n)h + \tilde{\theta}\mathbf{b}''(t_n)\tfrac{h^2}{2} + o(h^2); \end{aligned} \tag{37}$$

with $\tilde{\omega} = \tilde{c}_{-1} - \dfrac{\tilde{c}_1}{\nu} = \omega$ and $\tilde{\theta} = \tilde{c}_{-1} + \dfrac{\tilde{c}_1}{\nu^2}$. The local truncation error expressions (9), (10) and error estimates (35) and (36) still hold by replacing θ with $\tilde{\theta}$.

Remark 5.1 *From now on we will consider only second order time-adaptive predictors and correctors method. First order methods are used only in the first step, whose errors are estimated with (36). If we use CN* as a corrector, we have, for the first iteration, a first order predictor (FE*) and a second order corrector (CN*). In this case we cannot use the error estimates (35) nor (36). In order to adapt the first time-step, in the following simulations, we use for the first step the corrector scheme defined by coefficients* ($c_{-1} = 1$, $c_0 = 0$ *and* $c_1 = 0$) *(Backward Euler) in place of of the Crank-Nicolson one.*

We solved Luo-Rudy system with the time-adaptive algorithm, using different predictor-corrector methods fixed the predictor scheme to be the AB2* scheme. The corrector schemes are AM3*, CN* and M(0.6)* schemes. Results are shown in Table 6. M(0.6)* is more stable than CN^* but results show that performs slightly worst. In Figure 3 we compare the error curves as a function of the average step h, using the Rush-Larsen scheme, the AB2* scheme and the time adaptive algorithm with the AB2*-CN* scheme with PEC approach.

	AB2*-AM3*			AB2*-CN*			AB2*-M(0.6)*		
τ	h	r	err	h	r	err	h	r	err
2.5e-2	1.25	3%	4.18e-2	1.23	4%	3.65e-2	1.24	3%	3.91e-2
5e-3	7.29e-1	3%	3.21e-3	7.23e-1	3%	2.94e-3	7.25e-1	3%	3.44e-2
1e-3	4.27e-1	2%	2.18e-3	4.25e-1	3%	9.09e-4	4.24e-1	2%	4.90e-3
1e-4	1.99e-1	1%	5.58e-4	1.98e-1	1%	2.31e-4	1.97e-1	1%	5.58e-4
1e-5	9.25e-1	8‰	1.14e-4	9.19e-2	6‰	7.31e-5	9.17e-2	7‰	1.42e-4
1e-6	4.30e-1	6 ‰	2.43e-5	4.27e-2	3‰	1.96e-5	4.26e-2	2‰	3.64e-5

Table 6: Average time-step h, recomputed percentage r and relative error of the solution computed using different predictor-corrector methods with time adaptive strategy for different values of tolerance τ.

	AB2*-CN$^*_{PEC}$			AB2*-CN$^*_e$			AB2*-CN$^*_{e-PEC}$		
4 τ	h	r	err	h	r	err	h	r	err
2.5e-2	1.19	10%	3.10e-2	1.18	8%	2.51e-2	1.20	9%	2.22e-2
5e-3	7.22e-1	4%	3.54e-3	7.22e-1	4%	4.73e-3	7.22e-1	3%	7.28e-3
1e-3	4.25e-1	2%	1.38e-3	4.25e-1	2%	9.30e-4	4.25e-1	2%	2.75e-3
1e-4	1.98e-1	1%	2.25e-4	1.98e-1	1%	1.19e-4	1.98e-2	1e%	4.13e-4
1e-5	9.19e-2	7‰	5.50e-5	9.19e-2	7‰	1.48e-5	9.19e-2	7‰	4.79e-5
1e-6	4.27e-2	3‰	1.75e-5	4.27e-2	3‰	1.66e-6	4.27e-2	3‰	5.13e-6

Table 7: Average time-step h, recomputed percentage r and relative error of the solution computed using the predictor-corrector method AB2*-CN* with time adaptive strategy for different values tolerance τ. From left to right, the solution is computed respectively with a PEC approach, with a PECE approach and local extrapolation, with PEC approach and local extrapolation.

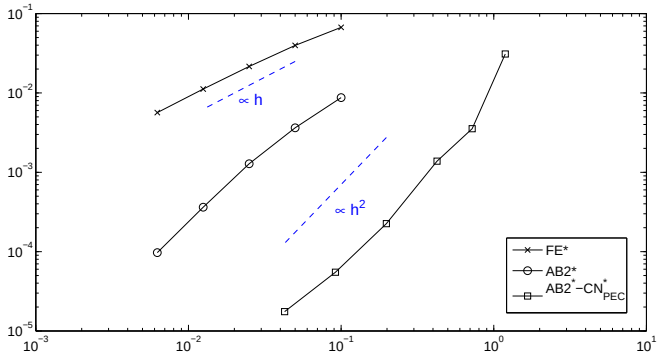

Figure 3: Relative error curves as a function of the average step h, using FE* scheme, AB2* scheme and the time adaptive algorithm with the AB2*-CN* scheme with PEC approach.

6 Monodomain and Bidomain systems

The Bidomain model is one of the most popular and accurate model to describe the propagation of action potential in the myocardium. A mathematical derivation of the Bidomain model is stressed in [7]. Well-posedness analysis results on Bidomain system coupled with different ionic model are presented in [20, 21], while several simulations of the action potential propagation using Monodomain and Bidomain systems can be found in [5] or [6]. Here we report the Bidomain system in a non-symmetric form:

$$\begin{cases} \dfrac{\partial u}{\partial t} - \dfrac{1}{\chi C_m}\nabla\cdot\left(\dfrac{\lambda \mathbf{D}_i}{1+\lambda}\nabla u\right) - \dfrac{1}{\chi C_m}\nabla\cdot\left(\dfrac{\lambda \mathbf{D}_i - \mathbf{D}_e}{1+\lambda}\nabla u^e\right) = I & \text{in } \Omega\times(0,T] \\ -\nabla\cdot[\mathbf{D}_i\nabla u + (\mathbf{D}_i+\mathbf{D}_e)\nabla u^e] = 0. & \text{in } \Omega\times(0,T] \\ \mathbf{n}^T\mathbf{D}_i(\nabla u + \nabla u^e) = 0 & \text{on } \partial\Omega\times(0,T], \\ \mathbf{n}^T\mathbf{D}_e\nabla u^e = \tilde{I}^{app} & \text{on } \partial\Omega\times(0,T], \\ \int_\Omega u^e d\mathbf{x} = 0 & \text{in } (0,T], \\ \dfrac{\partial \mathbf{X}}{\partial t} = \mathbf{g}(u,\mathbf{X},\mathbf{w}) & \text{in } \Omega\times(0,T] \\ \dfrac{\partial w_i}{\partial t} = a_i(u)w_i + b_i(u) & \text{in } \Omega\times(0,T] \\ u(\mathbf{x},0)=u_0,\ u^e(\mathbf{x},0)=0,\ \mathbf{X}(\mathbf{x},0)=\mathbf{X}_0,\ \mathbf{w}(\mathbf{x},0)=\mathbf{w}_0 & \text{in } \Omega, \end{cases} \tag{38}$$

where Ω is the spatial domain, u^e is the extracellular potential, $\mathbf{D}^i$ and $\mathbf{D}^e$ are the intracellular and extracellular conductivity tensors and χ the membrane area per unit tissue. The source terms $\tilde{I}_{app}$ and I are defined respectively as $\tilde{I}^i_{app} = I^i_{app} + I^e_{app}$ and $I = \dfrac{1}{C_m}\left(\dfrac{\lambda I^i_{app} - I^e_{app}}{\lambda+1} - I_{ion}\right)$, being I^i_{app} and I^e_{app} the applied intracellular and the extracellular current stimuli. The current stimuli must satisfy the compatibility condition $\int_\Omega (I^i_{app} + I^e_{app})\, d\mathbf{x} = 0$. In the sequel we take $I^i_{app} = -I^e_{app} = I^{app}$. Coefficient λ is a chosen in such a way that $\lambda\mathbf{D}_i \simeq \mathbf{D}_e$ in order to weaken the coupling between the first and the second equation. In the unrealistic case in which the conductivity tensors $\mathbf{D}_i$ and $\mathbf{D}_e$ are proportional, the Bidomain system can be reduced to the Monodomain system, and u^e has

not to be computed. The Monodomain system reads

$$\begin{cases} \dfrac{\partial u}{\partial t} - \dfrac{1}{\chi C_m}\nabla \cdot (\mathbf{D}^M \nabla u) = I & \text{in } \Omega \times (0,T] \\ \mathbf{n}^T \mathbf{D}^M \nabla u = 0 & \text{on } \partial\Omega \times (0,T], \\ \dfrac{\partial \mathbf{X}}{\partial t} = \mathbf{g}(u, \mathbf{X}, \mathbf{w}) & \text{in } \Omega \times (0,T] \\ \dfrac{\partial w_i}{\partial t} = a_i(u)\mathbf{w}_i + b_i(u) & \text{in } \Omega \times (0,T] \\ u(\mathbf{x},0) = u_0,\ \mathbf{X}(\mathbf{x},0) = \mathbf{X}_0,\ \mathbf{w}(\mathbf{x},0) = \mathbf{w}_0 & \text{in } \Omega; \end{cases} \tag{39}$$

where $D^M = \dfrac{\lambda \mathbf{D}_i}{1+\lambda}$ is the conductivity tensor and I is defined as: $I = \dfrac{1}{C_m}(I_{app} - I_{ion})$.

6.1 Monodomain model discretization

In the time discretization of (39) we treat implicitly the diffusion term in order to avoid small time-steps. Usually, Monodomain system is discretized as follows :

$$\begin{cases} \frac{1}{h}u^{n+1} - \nabla \cdot (\mathbf{D}^M \nabla u^{n+1}) = \frac{1}{h}u^n + I^n \\ \frac{1}{h}w_i^{n+1} = \frac{1}{h}w_i^n + \Phi(a_i^n h)\,(a_i^n w_i^n + b_i^n) \quad i = 1, \dots, m \\ \frac{1}{h}\mathbf{X}^{n+1} = \frac{1}{h}\mathbf{X}^n + \mathbf{g}^n; \end{cases} \tag{40}$$

for $n = 0, \dots, N$. The PDE is solved with an IMEX [11] method that combines Backward Euler (BE) with FE. The gate variables are solved with Rush-Larsen model, and concentration variables with FE. We call this method IMEX-FE*. A slight improvement of IMEX-FE* method consists in replacing, in the first equation, I^n with $I(u^n, \mathbf{w}^{n+1}, \mathbf{X}^{n+1})$. Since this is similar to a Gauss-Seidel substitution approach, we call this method IMEX-FE*-GS. A second order scheme can be achieved using the AB2* scheme for the gate equations, AB2 for the concentration equations and a second order IMEX scheme for the PDEs. We choose as IMEX scheme the combination of CN scheme for the diffusion term and AB2 for the forcing term. In this case the discrete system reads

$$\begin{cases} \frac{1}{h}u^{n+1} - \frac{1}{2}\nabla \cdot (\mathbf{D}^M \nabla u^{n+1}) = \frac{1}{h}u^n + \frac{1}{2}\nabla \cdot (\mathbf{D}^M \nabla u^n) + \frac{3}{2}I^n - \frac{1}{2}I^{n-1} \\ \frac{1}{h}w_i^{n+1} = \frac{1}{h}w_i^n + \Phi(a_i^{n+\frac{1}{2}}h)\left(a_i^{n+\frac{1}{2}}w_i^n + b_i^{n+\frac{1}{2}}\right) \quad i = 1, \dots, m \\ \frac{1}{h}\mathbf{X}^{n+1} = \frac{1}{h}\mathbf{X}^n + \frac{3}{2}\mathbf{g}^n - \frac{1}{2}\mathbf{g}^{n-1} \end{cases} \tag{41}$$

for $n = 1, \dots, N$, where we set $I^{n-1} = I^n$, $\mathbf{g}^{n-1} = \mathbf{g}^n$ and $\boldsymbol{a}^{n+\frac{1}{2}}$, $\boldsymbol{b}^{n+\frac{1}{2}}$ are chosen as in (7) with $c_{-1} = 0$, $c_0 = \frac{3}{2}$ and $c_1 = -\frac{1}{2}$.
This scheme becomes unstable for time-steps greater than 1 ms and oscillations persist for time-steps greater than 0.5 ms. In order to overcame these problems

and reduce at the same time computational efforts we apply our time adaptive scheme. We still treat implicitly the diffusion term also in the predictor-corrector scheme. This procedure does not affect the error estimate, since (9), (10), (35), (36) still hold. The entire time discretized Monodomain problem reads

$$
\begin{aligned}
P:\ &\begin{cases}
\frac{1}{h}\hat{u}^{n+1} = \frac{1}{h}u^n - \overline{c}_0\,\nabla\cdot(\mathbf{D}^M\nabla u^n) - \overline{c}_1\,\nabla\cdot(\mathbf{D}^M\nabla u^{n-1}) + \overline{c}_0\,I^n + \overline{c}_1\,I^{n-1} \\
\frac{1}{h}\hat{w}_i^{n+1} = \frac{1}{h}w_i^n + \Phi(\overline{a}_i^{n+\frac{1}{2}}h)\left(\overline{a}_i^{n+\frac{1}{2}}w_i^n + \overline{b}_i^{n+\frac{1}{2}}\right) \quad i=1,\dots,m \\
\frac{1}{h}\hat{\mathbf{X}}^{n+1} = \frac{1}{h}\mathbf{X}^n + \overline{c}_0\,\mathbf{g}^n + \overline{c}_1\,\mathbf{g}^{n-1}
\end{cases} \\
C:\ &\begin{cases}
\frac{1}{h}u^{n+1} - c_{-1}\,\nabla\cdot(\mathbf{D}^M\nabla u^{n+1}) = \\
\quad \frac{1}{h}u^n + c_0\nabla\cdot(\mathbf{D}^M\nabla u^n) + c_1\nabla\cdot(\mathbf{D}^M\nabla u^{n-1}) + c_{-1}\hat{I}^{n+1} + c_0 I^n + c_1 I^{n-1} \\
\frac{1}{h}w_i^{n+1} = \frac{1}{h}w_i^n + \Phi\big(\hat{a}_i^{n+\frac{1}{2}}h\big)\left(\hat{a}_i^{n+\frac{1}{2}}\,w_i^n + \hat{b}_i^{n+\frac{1}{2}}\right) \quad i=1,\dots,m \\
\frac{1}{h}\mathbf{X}^{n+1} = \frac{1}{h}\mathbf{X}^n + c_{-1}\hat{\mathbf{g}}^{n+1} + c_0\mathbf{g}^n + c_1\,\mathbf{g}^{n-1};
\end{cases}
\end{aligned}
\tag{42}
$$

for $n=1,\dots,N$, where $\hat{I}^{n+1}$ and $\hat{\mathbf{g}}^{n+1}$ are computed using the predictor solutions $\hat{u}^{n+1}$, $\hat{\mathbf{w}}^{n+1}$, $\hat{\mathbf{X}}^{n+1}$ and $\overline{\boldsymbol{a}}^{n+\frac{1}{2}}$, $\overline{\boldsymbol{b}}^{n+\frac{1}{2}}$, $\overline{\boldsymbol{a}}^{n+\frac{1}{2}}$ and $\overline{\boldsymbol{a}}^{n+\frac{1}{2}}$ are defined as in (31). We solve system (30) for the 1D Luo-Rudy model. Space discretization is carried out with a Galerkin linear finite element method. This choice is motivated in view of extending these computations to the 3D case. We consider $\Omega=(0,\,l)$ and introduce the grid points $\{x_k\}_0^{N_e}$ given by $x_k = k\,\delta x$, being $\delta x = \frac{l}{N_e}$ the grid spacing. We approximate y_i^n with $(y_h^n)_i = \sum_{k=0}^{N_e}\tilde{y}_{i,k}^n\varphi_k$ being $\{\varphi_k\}_0^{N_e}$ the Lagrangian base for the space of piecewise linear continuous functions on Ω. We define the 1D $L^2(\Omega)$ norm with a trapezoidal rule, namely

$$
\|(y_h^n)_i\| = \sqrt{\frac{1}{2}\sum_{k=0}^{M-1}\left[\left(\tilde{y}_{i,k}^n\right)^2 + \left(\tilde{y}_{i,k+1}^n\right)^2\right]\delta x}.
$$

We refer then to the space-time norm $\|(y_h^n)_i\|_{st} = \|\|(y_h^n)_i\|\|$. The relative error is given by $\max_i \dfrac{\|(y_h^n)_i - y_i(x_k,\,t^n)\|_{st}}{\|y_i(x_k,\,t^n)\|_{st}}$. Unless stated otherwise, in the following simulations we take $T=500$, $l=5cm$, $N_e=500$ and

$$
I_{app}(t,x) = \begin{cases} I_{max}\left(\frac{1}{2} - \frac{1}{2}\cos\left(2\pi\frac{t}{t_p}\right)\right) & t<t_p,\ x<x_p \\ 0 & \text{otherwise,} \end{cases}
\tag{43}
$$

where $I_{max}=60\mu A$, $t_p=1ms$ and $x_p=1.5mm$. We consider, as the reference solution, the one obtained using the predictor-corrector scheme AB2*-CN*, adapted in time, with $\tau = 1e-9$ and $N_e=500$. We are interested only in time discretization errors, hence, the reference solution is computed on the same grid used for the other numerical solutions. In Table 8 we report results obtained for different time-steps, using IMEX-FE*, IMEX-FE*-GS and IMEX-AB2* schemes. In Table 9 we report results obtained with the AB2*-CN* scheme and the predictor-corrector scheme AB2*-M(0.6)*. In Figure 4 we report rel-

h	IMEX-FE*	IMEX-FE*-GS	IMEX-AB2*
2e-1	4.47e-1	5.14e-2	`NaN`
1e-1	3.09e-1	6.85e-2	4.67e-2
5e-2	2.12e-1	5.71e-2	4.24e-2
2.5e-2	1.48e-1	3.71e-2	1.86e-2
1.25e-2	1.02e-1	2.17e-2	5.52e-3
6.25e-3	6.59e-2	1.18e-2	1.46e-3

Table 8: Relative errors using different time-steps and the methods IMEX-FE*, IMEX-FE*-GS and IMEX-AB2*. The results in the first two columns refer to the PECE approach, while in the last two columns to the PEC approach.

	AB2*-CN*			AB2*-CN$^*_{PEC}$			AB2*-M(0.6)$^*_{PEC}$		
τ	h	r	err	h	r	err	h	r	err
1e-1	5.92e-1	1%	2.57e-1	4.78e-1	7%	1.71e-1	4.87e-1	28%	9.53e-2
2.5e-2	3.63e-1	6‰	3.96e-2	3.43e-1	9‰	4.04e-2	3.42e-1	15%	3.19e-2
5e-3	2.14e-1	6‰	2.90e-2	2.11e-1	8‰	2.70e-2	2.14e-1	7‰	2.13-2
1e-3	1.26e-1	6‰	1.34e-2	1.26e-1	5‰	1.30e-2	1.24e-1	13%	1.10e-2
1e-4	5.70e-2	11%	3.14e-3	5.77e-2	7%	3.06e-3	5.53e-2	17%	2.67e-3
1e-5	2.62e-2	11%	6.21e-4	2.62e-2	10%	6.20e-4	2.55e-2	17%	6.13e-4

Table 9: Average time-step h, recomputed percentage r and relative error of the solution of Monodomain model, computed using different predictor-corrector methods with time adaptive strategy.

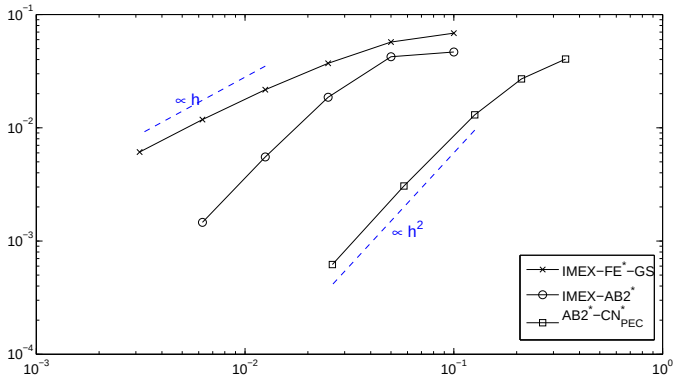

Figure 4: Relative error curves as a function of the average step h, using IMEX-FE* scheme, IMEX-AB2* scheme and the time adaptive algorithm with the AB2*-CN* scheme with PEC approach.

	AB2*-CN*$_{PEC}$, $\delta x = \frac{5}{125}$			AB2*-CN*$_{PEC}$, $\delta x = \frac{5}{250}$			AB2*-CN*$_{PEC}$, $\delta x = \frac{5}{500}$		
τ	h	r	err	h	r	err	h	r	err
1e-1	5.18e-1	30%	1.57e-1	4.80e-1	18%	2.11e-1	4.78e-1	7%	1.71e-1
2.5e-2	3.58e-1	27%	5.97e-2	3.55e-1	16%	3.11e-2	3.43e-1	9‰	4.04e-2
5e-3	2.21e-1	22%	5.32e-2	2.15e-1	9‰	3.56e-2	2.11e-1	8‰	2.70e-2
1e-3	1.31e-1	10%	2.30e-2	1.27e-1	8‰	1.65e-2	1.26e-1	5‰	1.30e-2
1e-4	6.10e-2	8%	3.69e-3	5.89e-2	3%	3.56e-3	5.77e-2	7%	3.06e-3
1e-5	2.82e-2	4%	5.33e-4	2.71e-2	5%	6.77e-4	2.62e-2	10%	6.20e-4

Table 10: Average time-step h, recomputed percentage r and relative error of the solution of Monodomain model, computed on different grids, using AB2*-CN*$_{PEC}$ scheme with time adaptive strategy.

ative error curves as a function of the average time-step h, using IMEX-FE* scheme, IMEX-AB2* scheme and the time adaptive algorithm with the AB2*-CN* scheme. Second order methods with $\theta < \frac{1}{2}$ used as correctors and methods corrected with local extrapolation present instabilities.
The numerical methods is robust with respect to the spatial resolution as shown in Table 10 where we compare the average time-step h, the recomputed percentage r and the relative error for different mesh sizes. The reference solutions are computed using the different grids and taking a tolerance defined as $\tau = 1e-9$. The recomputed percentage increases on coarse grids, while h and the errors are fairly insensitive.

Remark 6.1 The 3D Bidomain problem.

A complete analysis of the results of our solver coupled with the (2D-3D)

Bidomain complete model is beyond the scope of the present work. However, we want to address briefly a possible strategy for an efficient coupling of the PDE solver and our method. Usually, the Bidomain system is written in a symmetric form featuring the two variables u^i and u^e, where $u^i = u + u^e$ is the intracellular potential. However, if we resort to the non-symmetric form, in the predictor step we avoid to solve the second equation of the system. The time discretized problem reads, for $n = 1, \ldots, N$

$$
\begin{cases}
\frac{1}{h}\hat{u}^{n+1} = \frac{1}{h}u^n + \overline{c}_0\,\nabla\cdot(\mathbf{D}^M\nabla u^n) + \overline{c}_1\,\nabla\cdot(\mathbf{D}^M\nabla u^{n-1}) + \\
\qquad \overline{c}_0\,\nabla\cdot(\mathbf{D}^\Delta\nabla(u^e)^n) + \overline{c}_1\,\nabla\cdot(\mathbf{D}^\Delta\nabla(u^e)^{n-1}) + \overline{c}_0\,I^n + \overline{c}_1\,I^{n-1} \\
\frac{1}{h}\hat{w}_i^{n+1} = \frac{1}{h}w_i^n + \Phi(\overline{a}_i^{n+\frac{1}{2}}h)\left(\overline{a}_i^{n+\frac{1}{2}}\,w_i^n + \overline{b}_i^{n+\frac{1}{2}}\right) \\
\frac{1}{h}\hat{\mathbf{X}}^{n+1} = \frac{1}{h}\mathbf{X}^n + \overline{c}_0\,\mathbf{g}^n + \overline{c}_1\,\mathbf{g}^{n-1}
\end{cases}
$$

$$
C:\ \begin{cases}
\frac{1}{h}u^{n+1} - c_{-1}\,\nabla\cdot(\mathbf{D}^M\nabla u^{n+1}) - c_{-1}\,\nabla\cdot(\mathbf{D}^\Delta\nabla(u^e)^{n+1}) = \\
\qquad \frac{1}{h}u^n + c_0\nabla\cdot(\mathbf{D}^M\nabla u^n) + c_1\nabla\cdot(\mathbf{D}^M\nabla u^{n-1}) + c_0\nabla\cdot(\mathbf{D}^\Delta\nabla(u^e)^n) + \\
\qquad c_1\nabla\cdot(\mathbf{D}^\Delta\nabla(u^e)^{n-1}) + c_{-1}\hat{I}^{n+1} + c_0 I^n + c_1 I^{n-1} \\
-\nabla\cdot\left[\mathbf{D}_i\nabla u^{n+1} + (\mathbf{D}_i + \mathbf{D}_e)\nabla(u^e)^{n+1}\right] = 0 \\
\int_\Omega (u^e)^{n+1} d\mathbf{x} = 0 \\
\frac{1}{h}w_i^{n+1} = \frac{1}{h}w_i^n + \Phi\left(\hat{a}_i^{n+\frac{1}{2}}h\right)\left(\hat{a}_i^{n+\frac{1}{2}}\,w_i^n + \hat{b}_i^{n+\frac{1}{2}}\right) \\
\frac{1}{h}\mathbf{X}^{n+1} = \frac{1}{h}\mathbf{X}^n + c_{-1}\hat{\mathbf{g}}^{n+1} + c_0\mathbf{g}^n + c_1\,\mathbf{g}^{n-1},
\end{cases}
\tag{44}
$$

where $D^M = \frac{\lambda\mathbf{D}_i}{1+\lambda}$ and $D^\Delta = \frac{\lambda\mathbf{D}_i - \mathbf{D}_e}{1+\lambda}$. The terms $\hat{I}^{n+1}$, $\hat{\mathbf{g}}^{n+1}$, $\overline{\boldsymbol{a}}^n$, $\overline{\boldsymbol{b}}^n$, $\hat{\boldsymbol{a}}^n$, $\hat{\boldsymbol{b}}^n$ are defined as in the system (42).

Most of the computational effort is required by the solution of the PDEs system in the corrector step. An efficient way to solve this system is presented in [8]. A detailed analysis of 3D Bidomain results with our method will be presented elsewhere (see [15]).

7 Conclusions

We presented the generalization to the popular Rush-Larsen method used for solving nonlinear ordinary differential systems for the ionic dynamics in electrophysiology, in particular for the cardiac potential propagation. We extended the method to a class of second order schemes. These can be regarded also a generalization of classical multistep methods whenever the problem at hand is naturally split into a part where it is worth to put in evidence a linear dependence on the unknown and the remainder of the nonlinear terms. We have carried out the analysis of the schemes, including the Rush-Larsen one which at the best of our knowledge was never analyzed so far. One of the relevant properties of these methods is that they can preserve bounds on the solution that guarantee that the physical significance of the unknown is preserved. Moreover, analysis shows that the approach pursued here introduces an improvement of the absolute

stability properties of the corresponding multistep scheme, as numerical results confirm. This goes beyond the specific applications that have originated this work, suggesting that an appropriate splitting of any problem at hand can be faced with a method of our class $\mathrm{M}^*(\theta)$ with larger time steps respect to the multistep $\mathrm{M}(\theta)$. The major limitation of this approach is the accuracy, that at the moment is limited to the second order.

We presented an extensive discussion on the predictor corrector formulation of our method for the problems in electro-physiology and the consequent time-adaptive implementation, which is of paramount relevance in cardiac applications. Preliminary results carried out on a simplified 1D model for cardiac potential confirm the effectiveness of our approach in view of more realistic simulations over 3D domains.

Appendix

We report Luo-Rudy model phase I [14]. Variables $\mathbf{w}$, $\mathbf{X}$ and functions I, $\boldsymbol{a}$, $\boldsymbol{b}$ and $\mathbf{g}$ of system (1) are specified as follows. We made slightly modifications on the original model in functions α_h, β_h, α_j, β_j and X_i in order to make them continuous. Modifications regards only the inequalities on u.

$\mathbf{w} = [h\ j\ m\ d\ f\ X]^T$,
$\boldsymbol{a} = -[(\alpha_h + \beta_h),\ (\alpha_j + \beta_j),\ (\alpha_m + \beta_m),\ (\alpha_d + \beta_d),\ (\alpha_f + \beta_f),\ (\alpha_X + \beta_X)]^T$,
$\boldsymbol{b} = [\alpha_h\ \alpha_j\ \alpha_m\ \alpha_d\ \alpha_f\ \alpha_X]^T$,
$\mathbf{X} = [Ca], \quad \mathbf{g} = -10^{-4} I_{si} + 0.07(10^{-4} - Ca)$,
$I_{ion} = I_{K1} + I_{K_p} + I_b + I_K + I_{Na} + I_{si}$,
$u_0 = -84mV, \quad \mathbf{X}_0 = 2e-4mM, \quad \mathbf{w}_0 = [1\,1\,0\,0\,1\,0]^T$,

where the gating functions are defined as follows:

$$I_{Na} = 23\, m^3\, h\, j\, (u - E_{Na}), \qquad E_{Na} = 54.4mV$$

$$\alpha_h = 0.135e^{-\frac{80+u}{6.8}}$$

$$\beta_h = \begin{cases} 0.13\left(1 + e^{-\frac{u+10.66}{11.1}}\right) & u \geq -38.7381 \\ 3.56e^{0.079u} + 3.1 \cdot 10^5 e^{0.35u} & u < -38.7381 \end{cases}$$

$$\alpha_j = \begin{cases} \dfrac{(u + 37.78)\left(-1.2714 \cdot 10^5\, e^{0.2444u} - 3.474 \cdot 10^{-5}\, e^{-0.04391u}\right)}{1 + e^{0.311(u+79.23)}} & u < -37.78 \\ 0 & u \geq -37.78 \end{cases}$$

$$\beta_j = \begin{cases} \dfrac{0.3e^{2.535 \cdot 10^{-7} u}}{1 + e^{-0.1(u+32)}} & u \geq -39.826 \\ \dfrac{0.1212e^{-0.01052u}}{1 + e^{-0.1378(u+40.14)}} & u < -39.826 \end{cases}$$

$$\alpha_m = 0.32\frac{u + 47.13}{1 - e^{-0.1(u+47.13)}} \qquad \beta_m = 0.08e^{-\frac{u}{11}}$$

$$\alpha_d = 0.095\frac{e^{-0.01(u-5)}}{1 + e^{-0.072(u-5)}}, \qquad \beta_d = 0.07\frac{e^{-0.017(u+44)}}{1 + e^{0.05(u+44)}}$$

$$\alpha_f = 0.012\frac{e^{-0.008(u+28)}}{1 + e^{0.15(u+28)}}, \qquad \beta_f = 0.0065\frac{e^{-0.02(u+30)}}{1 + e^{-0.2(u+30)}}$$

$$\alpha_X = 0.0005\frac{e^{0.083(u+50)}}{1 + e^{0.057(u+50)}}, \qquad \beta_X = 0.0013\frac{e^{-0.06(u+20)}}{1 + e^{-0.04(u+20)}}.$$

Ionic currents are defined as follows:

$$I_{si} = 0.09\, d\, f(u - E_{si}),$$

$$E_{si} = 7.7 - 13.0287\ln(Ca),$$

$$I_K = \overline{G_K} X X_i (u - E_K),\ E_K = -77.01mV,\ \overline{G}_K = 0.282\sqrt{\tfrac{K_o}{5.4}},\ K_o = 5.4mM,$$

$$X_i = \begin{cases} 2.837\dfrac{e^{0.04(u+77)} - 1}{(u + 77)e^{0.04(u+35)}} & u > -100.05, \\ 1 & u \leq -100.05, \end{cases}$$

$$I_{K1} = \overline{G}_{K1}\frac{\alpha_{K1}}{\alpha_{K1} + \beta_{K1}}(u - E_{K1}), \quad E_{K1} = -87.26mV, \qquad \overline{G}_{K1} = 0.282\sqrt{\tfrac{K_0}{5.4}},$$

$$\alpha_{K1} = 1.02\frac{1}{1 + e^{0.2385(u - E_{K1} - 59.215)}},$$

$$\beta_{K1} = \frac{0.49124e^{0.08032(u - E_{K1} + 5.476)} + e^{0.06175(u - E_{K1} - 594.31)}}{1 + e^{-0.5143(u - E_{K1} + 4.753)}},$$

$$I_{K_p} = 0.0183K_p(u - E_{Kp}), \qquad E_{Kp} = E_{K1},$$

$$K_p = \frac{1}{1 + e^{\frac{7.488 - u}{5.98}}},$$

$$I_b = 0.03921(u + 59.87),$$

Acknowledgments

The authors thank Marta D'Elia for her helpful comments in preparing this work.

References

[1] G. W. Beeler and H. Reuter, *Reconstruction of the action potential of ventricular myocardial fibres*, The Journal of Physiology, 268 (1977), p. 177210. PMC1283659.

[2] E. M. Cherry, H. S. Greenside, and C. S. Henriquez, *A space-time adaptive method for simulating complex cardiac dynamics*, Physical Review Letters, 84 (2000), pp. 1343–1346.

[3] M. Courtemanche, R. J. Ramirez, and S. Nattel, *Ionic mechanisms underlying human atrial action potential properties: insights from a mathematical model*, The American Journal of Physiology, 275 (1998), pp. H301–21. PMID: 9688927.

[4] P. C. Franzone, P. Deuflhard, B. Erdmann, J. Lang, and L. F. Pavarino, *Adaptivity in space and time for reaction-diffusion systems in electrocardiology*, SIAM J. Sci. Comput., 28 (2006), pp. 942–962.

[5] P. C. Franzone and L. F. Pavarino, *A parallel solver for reaction-diffusion systems in computational electrocardiology*, Mathematical models and methods in applied sciences, 14 (2004), pp. 883–911.

[6] P. C. Franzone, L. F. Pavarino, and B. Taccardi, *Simulating patterns of excitation, repolarization and action potential duration with cardiac bidomain and monodomain models*, Math. Biosc., 197 (2005), pp. 35–66.

[7] P. C. Franzone and G. Savaré, *Degenerate evolution systems modeling the cardiac electric field at micro and macroscopic level*, Birkhauser, 2002, pp. 218–240.

[8] L. Gerardo-Giorda, L. Mirabella, F. Nobile, M. Perego, and A. Veneziani, *A model-based block-triangular preconditioner for the bidomain system in electrocardiology*, submitted, (2008).

[9] A. L. Hodgkin and A. F. Huxley, *A quantitative description of membrane current and its application to conduction and excitation in nerve*, The Journal of Physiology, 117 (1952), pp. 500–44. PMID: 12991237.

[10] W. Hundsdorfer, S. J. Ruuth, and R. J. Spiteri, *Monotonicity-preserving linear multistep methods*, SIAM Journal on Numerical Analysis, 41 (2003), pp. 605–623.

[11] W. Hundsdorfer and J. Verwer, *Numerical Solution of Time-Dependent Advection-Diffusion-Reaction Equations*, vol. 33 of Springer Series in Computational Mathematics, Springer, 2003.

[12] M. S. Jafri, J. J. Rice, and R. L. Winslow, *Cardiac ca2+ dynamics: the roles of ryanodine receptor adaptation and sarcoplasmic reticulum load*, Biophysical Journal, 74 (1998), pp. 1149–68. PMID: 9512016.

[13] J. D. Lambert, *Numerical Methods For Ordinary Differential Systems*, John Wiley & Sons, 1991.

[14] L. Luo and Y. Rudy, *A model of the ventricular cardiac action potential: depolarization, repolarization and their interaction*, Circulation Research, 68 (1991).

[15] M. Perego, *Mathematical and Numerical Models for Focal Cerebral Ischemia and Electrocardiology*, PhD thesis, Politecnico di Milano, 2009.

[16] A. J. Pullan, L. K. Cheng, M. L. Buist, and M. L. B. Andrew J. Pullan, Leo K. Cheng, *Mathematically Modelling the Electrical Activity of the Heart*, Wolrd Scientific, 2005.

[17] A. Quarteroni, R. Sacco, and F. Saleri, *Numerical Mathematics*, Springer, Apr. 2000.

[18] S. Rush and H. Larsen, *A practical algorithm for solving dynamic membrane equations*, Biomedical Engineering, IEEE Transactions on, BME-25 (1978), pp. 389–392.

[19] J. Sundnes, G. T. Lines, and A. Tveito, *An operator splitting method for solving the bidomain equations coupled to a volume conductor model for the torso*, Mathematical biosciences, 194 (2005), p. 233248.

[20] M. Veneroni, *Reaction-diffusion systems for the microscopic cellular model of the cardiac electric field*, Math. Method Appl. Sci., 29 (2006), pp. 1631–1661.

[21] ——, *Reaction-diffusion systems for the macroscopic bidomain model of the cardiac electric field*, Nonlinear Analysis: Real World Applications, 10 (2009), pp. 849–868.

[22] H. Yu, *A local space-time adaptive scheme in solving two-dimensional parabolic problems based on domain decomposition methods*, SIAM J. Sci. Comput., 23 (2001), pp. 304–322.

MOX Technical Reports, last issues

Dipartimento di Matematica "F. Brioschi",
Politecnico di Milano, Via Bonardi 9 - 20133 Milano (Italy)

07/2009 M. Perego, A. Veneziani:
An efficient generalization of the Rust-Larsen method for solving electrophysiology membrane equations

06/2009 L. Formaggia, A. Veneziani, C. Vergara:
Numerical solution of flow rate boundary for incompressible fluid in deformable domains

05/2009 F. Ieva, A.M. Paganoni:
A case study on treatment times in patients with ST-Segment Elevation Myocardial Infarction

04/2009 C. Canuto, P. Gervasio, A. Quarteroni:
Finite-Element Preconditioning of G-NI Spectral Methods

03/2009 M. D'Elia, L. Dedé, A. Quarteroni:
Reduced Basis Method for Parametrized Differential Algebraic Equations

02/2009 L. Bonaventura, C. Biotto, A. Decoene, L. Mari, E. Miglio:
A couple ecological-hydrodynamic model for the spatial distribution of sessile aquatic species in thermally forced basins

01/2009 E. Miglio, C. Sgarra:
A Finite Element Framework for Option Pricing the Bates Model

28/2008 C. D'Angelo, A. Quarteroni:
On the coupling of 1D and 3D diffusion-reaction equations. Applications to tissue perfusion problems

27/2008 A. Quarteroni:
Mathematical Models in Science and Engineering

26/2008 G. Aletti, C. May, P. Secchi:
A Central Limit Theorem, and related results, for a two-randomly reinforced urn